We are committed to providing [accessible customer service](#).
If you need accessible formats or communications supports, please [contact us](#).

Nous tenons à améliorer [l'accessibilité des services à la clientèle](#).
Si vous avez besoin de formats accessibles ou d'aide à la communication, veuillez [nous contacter](#).

Airborne Magnetics and Radiometrics

26/11/2019

Prepared by:

Jason Ploeger, P.GEO
Canadian Exploration Services Limited

With contributions from:
Frank Ploeger, P.GEO
Melanie Postman, GIT

Prepared For:

Battery Mineral Resources Ltd.
Level 36, Governor Philip Tower,
1 Farrer Place Sydney NSW 2000, Australia

TABLE OF CONTENTS

LIST OF APPENDICES

APPENDIX I: PRECISION GEOSURVEYS LOGISTICS REPORT

LIST OF FIGURES AND TABLES

1. SURVEY OVERVIEW

1.1 PROJECT NAME

This project is known as the **White Reserve Project.**

1.2 CLIENT

Battery Mineral Resources Limited

Level 36
Governor Phillip Tower
1 Farer Place
Sydney
Australia

1.3 SUMMARY

The Battery Mineral Resources' (BMR) White Reserve project is comprised of 606 mining cell claims, totaling 12,764.1 hectares, in Willet, Barber, Banks, Speight, Whitson and Van Nostrand townships. The center of the project area is ~120 km northeast of Sudbury and 30 km south of Elk Lake, Ontario.

During the summer of 2018, BMR contracted Precision GeoSurveys to fly an airborne Magnetic and Radiometric over the White Reserve Project area.

All coordinates presented in this report are in UTM NAD83 Zone 17N.

1.4 SURVEY & PHYSICAL ACTIVITIES UNDERTAKEN

Work Performed	Dates
Airborne Magnetometer	July 11 to July 14, 2018

Table 1: Survey and Physical Activity Details

2. SURVEY LOCATION DETAILS

2.1 LOCATION

The center of the White Reserve project area is ~120km northeast of Sudbury and 30 km south of Elk Lake, Ontario. It is located in Willet, Barber, Banks, Speight, Whitson and Van Nostrand townships. Figure 1 shows the general location of the White Lake property.
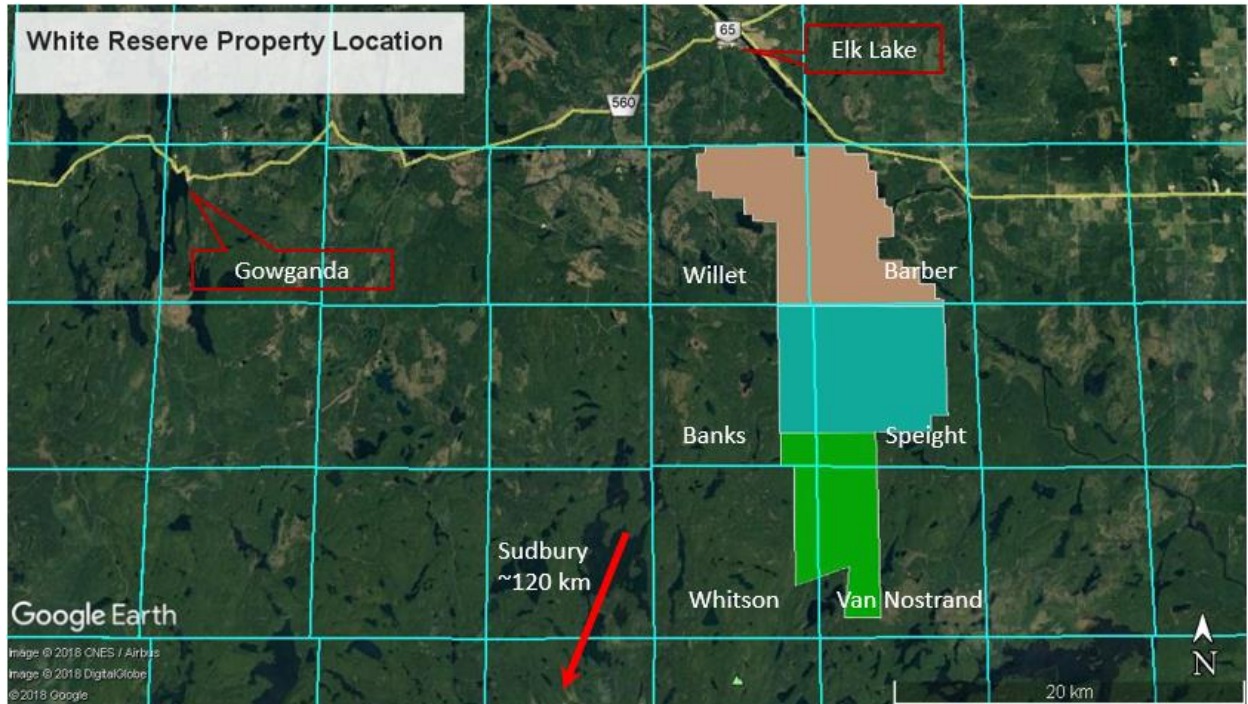

Figure 1:White Reserve Property Location Map

2.2 ACCESS

Access to the White Reserve property can be made by taking 6th Street southeast from Elk Lake for ~25 km to Little Spring Lake. From Little Spring Lake, a logging road can be taken south for ~5 km to the eastern edge of the White Reserve project claim boundary. From there, access can be made by ATV along pre-existing trails or by foot. See Figure 2 for detailed access routes.
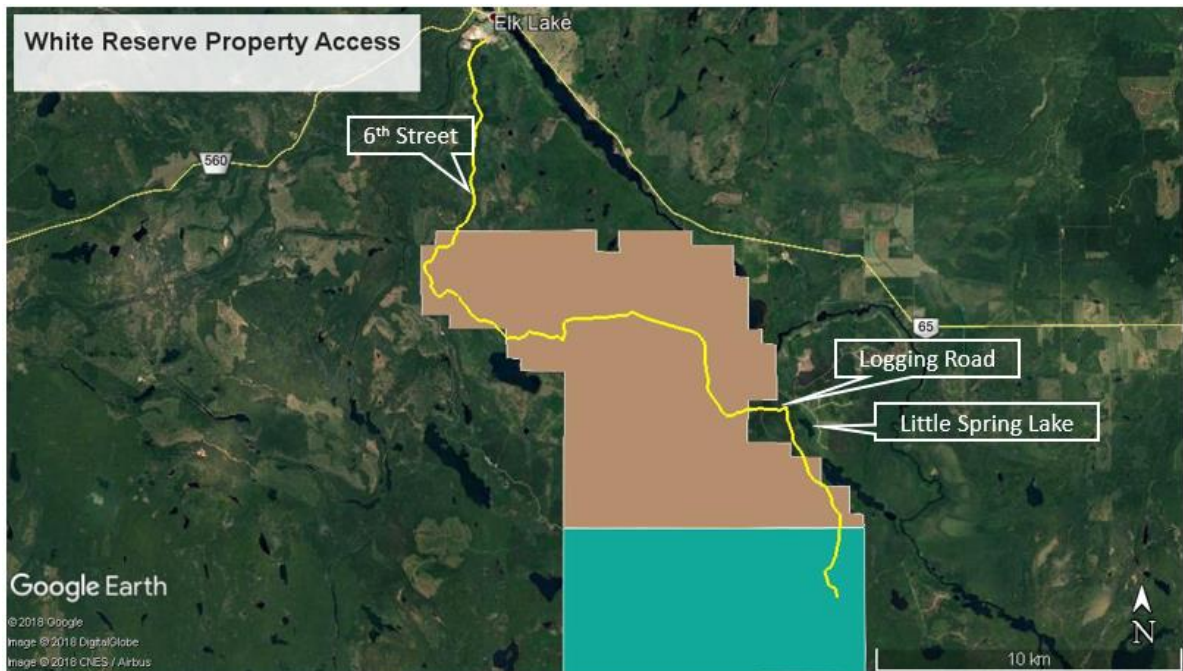

Figure 2: General Location and Access to the White Reserve Property

2.3 MINING CLAIMS / OWNERSHIP

The Battery Mineral Resources' (BMR) White Reserve project is comprised of 606 mining cell claims in Willet, Barber, Banks, Speight, Whitson and Van Nostrand townships, 30 km south of Elk Lake, Ontario. In total, BMR holds 12,764.1 hectares of semi-contiguous mining claims on this property. Mineral rights on the White Reserve property are held in two ways: a purchase agreement entered into on November 15, 2016 with Ashley Gold Mines Limited (20 claims) (Battery Mineral Resources, 2016) and claims staked and owned by BMR (586 claims).

A breakdown of the current tenure claims owned by Battery Mineral Resources on the property is listed in Appendix I and displayed in Figure 3.
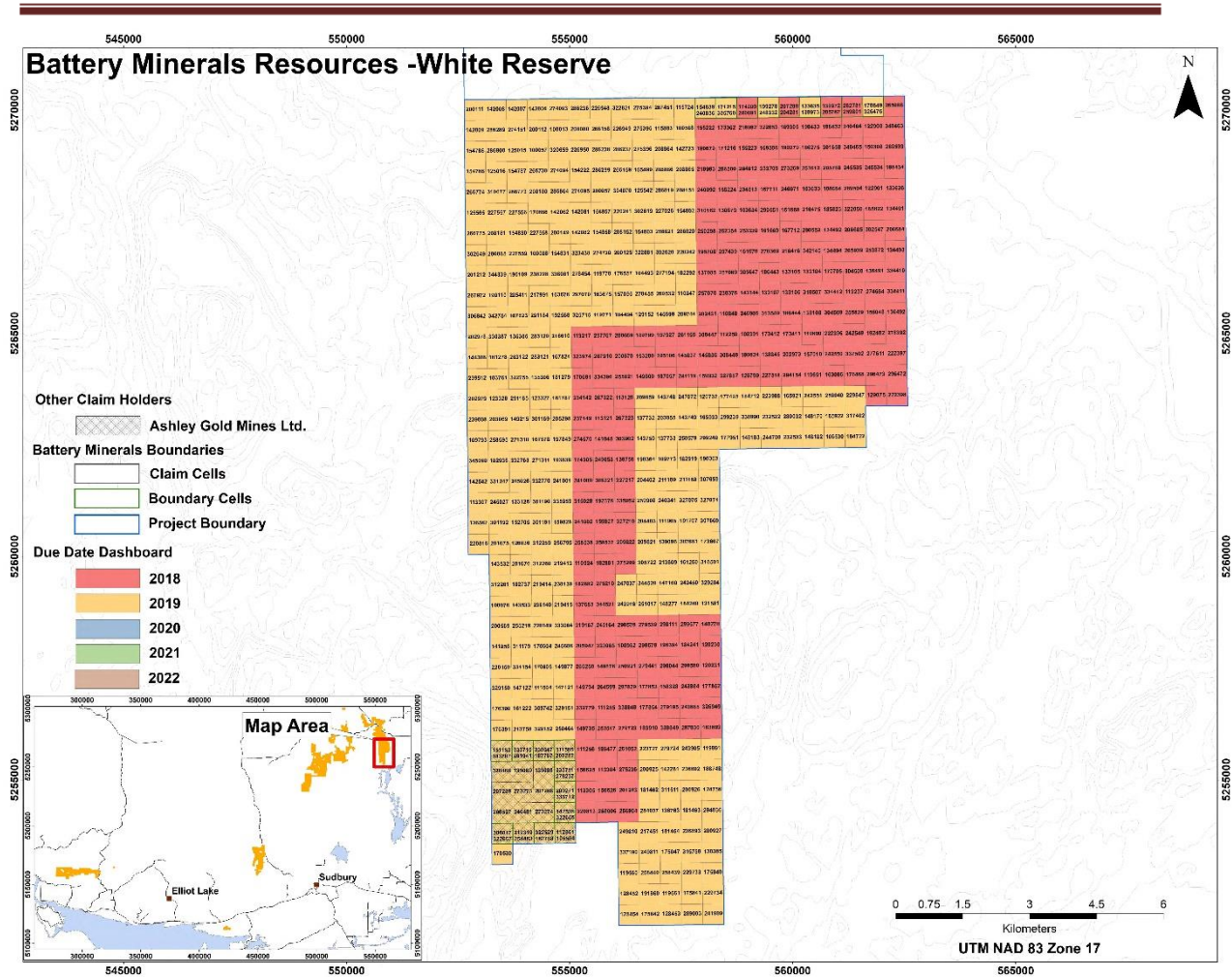
Figure 3: Mining cell claims comprising the White Reserve property.

2.4 PROPERTY & EXPLORATION HISTORY

1909-1910 White Reserve Mines:

The first record of work on the property included the sinking of one shaft to 147 feet with levels constructed at 70 and 140 feet, from 1909-1910, by White Reserves Mines (George, 1968). During this time, 35 feet of crosscuts and 100 feet of underground drifting were completed, and the company mined and shipped 5 tons of ore containing 18,002 oz of Ag (Rungis, 2008). Operations by White Reserve Mines ceased in 1910 (Rungis, 2008).

1914-1915 Unknown:

An additional 380 feet of cross cuts and 100 feet of drifting were completed under-

ground at the White Reserve Mine in 1914, and in 1915 another 200 feet of underground drifting was completed (George, 1968).

1919-1920 J.B. Tyrell:
J.B. Tyrell drew English interest to the property, which resulted in 800 feet of underground drilling, but no further work (George, 1968).

1934 Universal Gold Syndicates:
While prospecting the property twenty-four veins (variably Ag-mineralized) were discovered at surface and a Main Shaft was sunk to 147 feet, with levels constructed at 70 and 140 feet. Approximately 1,500 feet of crosscutting and drifting was completed on veins 7, 10, 14, and 21. Assay data from these and earlier mining efforts are vague, with few high assays and poor grade continuity reported (George, 1968). Overall, the drilled holes from early work were interpreted to be inadequately sampled (George, 1968).

1962 Union Miniere Exploration and Mining Corporation Limited.
The company contracted Canadian Aero Mineral Surveys Ltd. to conduct an aeromagnetic survey in the Anvil Lake area of the White Reserve property. Flight lines were north-directed, spaced 330 feet apart, and flown at a 250 foot nominal terrain clearance. A total of 317 line-miles of aeromagnetic data were collected. This data confirmed that the area surrounding Anviil Lake was primarily comprised of non-magnetic, Huronian metasedimentary rocks, intruded by magnetic Nipissing Diabase (Schuur, 1969).

1968: Union Miners Exploration Company (on Argentum Silver Mines property).
The company contracted Shield Geophysics Limited to conduct an exploration program on the White Reserve property. Reconnaissance mapping, detailed mapping, detailed geophysical surveys, a geochemical survey of the White Reserve Mine area, and a drilling program were completed. Following geological mapping, the area was prospected for veins in the Nipissing Diabase, with no new veins being discovered.

Ground EM and magnetic surveys were completed in selected portions of the claim area, mainly on north-oriented lines. Magnetometer readings were recorded at fifty foot intervals and EM readings were recorded at 25 foot intervals. Weak to moderate conductors were identified in some of the surveys and were generally interpreted to reflect geological features unrelated to the veins of economic interest. One conductor was outlined south of the old mill and was drill tested with hole 68-2. Magnetic data confirmed that the area was underlain by diverse and structurally modified rocks. However, there was little correlation between magnetic data anomalies and known mineralized zones.

Detailed mapping was completed to better understand the geology and controls on

mineralization across the property area. Grid mapping conducted using air-photos confirmed that host rocks were Nipissing Diabase that intruded Cobalt Group metasedimentary rocks. Observations revealed that the rocks form a west-dipping (15-20°) homocline, cross-cut by three generations of faults. Mineralized zones were determined to be narrow calcite veins that contained variable sulfide minerals of Ag, Bi, Cu, Ni, and Co, but no economically mineralized zones were discovered during mapping. Wall rocks in mineralized zone were often carbonate-rich and variably epidotized (George, 1968).

A bedrock geochemical survey was conducted on a preexisting grid, with samples collected every twenty-five feet to determine the distribution of Ag, Co, Ni, and Bi near the known mineralized zones. Two-hundred and eighty-one samples were collected and sent to Bondar-Clagg & Company Limited of Ottawa, Ontario. The samples were ground to -100 mesh size and analyzed using an atomic adsorption technique. Solution extraction was by HNO_3-HCL for Co, Ni, and Bi, and by HCL for Ag. Six areas containing anomalous metal values in one or more elements were identified in the survey, however no anomalies were considered significant proxies for large, low-grade Ag resources (George, 1968).

Five diamond drill holes were drilled to test areas thought to be prospective for large, low-grade Ag deposits based on mapping, geophysical, and geochemical survey data. Every hole cut Nipissing Diabase, and was drilled on surface-exposed Ag-mineralized zones. Alteration types were either K-feldspar, carbonate, or epidote-dominant. Only finely disseminated sulfides were intersected (diagenetic?), with no economically mineralized zones identified. Only relatively thin mineralized intervals (5 feet @ 1.6 oz/ton Ag) were identified, indicating little potential existed for a large, low-grade Ag deposit. Copper and nickel assays did not report values above background concentrations (George, 1968).

1970 Unknown:
A soil geochemistry program comprising 363 samples was conducted in the Speight Township portion of the White Reserve property (Wilson, 1970). Samples were collected from the "B" horizon and analyzed by Technical Service Laboratories of Toronto, Ontario, Canada. Only one sample from the initial survey contained highly anomalous concentrations of metals (16 ppm Ag and 450 ppm Co), with nearby follow up samples containing 1000 ppm and 160 ppm Ag. Anomalous Co values in soil samples were not interpreted to be representative the underlying geology (Wilson, 1970).

1970 Stanwick et al.:
One diamond drill hole (SK-1) was drilled in Speight Township and intercepted brecciated, veined, and variably mineralized diabase (Stanwick, 1971).

1971 Castlebar Silver and Cobalt:
The company drilled three diamond drill holes (C-71X-1, C-71X-2, C-71X-3) in

Speight Township that intercepted variably calcite (±sulfide) veined diabase (Castle-bar Silver and Cobalt, 1971).

1978 Charles Mortimer:
C. Mortimer completed a limited ground VLF and magnetic survey (Mortimer, 1999).

1999 Charles Mortimer:
L. Salo (under contract from C. Mortimer) completed a small prospecting program consisting of five, east-trending lines of magnetic and VLF data collection, as well as rock sample collection near Goldie Lake (Mortimer, 1999). The ground geophysical data outlined mutually exclusive conductors and mag anomalies that were not drill tested. Five rock samples were sent for assay—two from the shaft east of Goldie Lake, and three samples from the claim boundary—at Swastika Labs. The results showed that Au and Ag contents were at or near detection limits, and three samples contained anomalous Cu concentrations (0.411-.59%; Mortimer, 1999).

2005 Contact Diamond Corporation (CDC):
Following airborne geophysical surveying, CDC completed twenty-five ground based magnetic surveys over twenty-nine magnetic anomalies outlined in the previous airborne survey. The surveys, aimed at identifying kimberlite pipes, outlined several magnetic anomalies that resembled known kimberlite pipes (Long, 2005).

2006 Klondike Silver Corporation:
Klondike Silver Corp. contracted Katrine Exploration Services to conduct a GPS survey on the Anvil Property located partly in Speight, Van Nostrand, Whitson, and Banks Townships (Rungis, 2008). During this survey UTM coordinates of the historic mines, shafts and mining equipment were marked (Rungis, 2008).

2006 Temex Resources Corporation:
Temex contracted Fugro Airborne Surveys to conduct airborne magnetic surveys over parts of the Cobalt region in Ontario, including one survey (Block 1) that partially covered the White Reserve property. The helicopter survey comprised north-oriented flight lines, spaced 75 meters apart, and flown at 30 m nominal terrain clearance. Tie lines were flown orthogonal to the main flight lines, and were spaced 1000 m apart. A dual-senor MIDAS optically pumped cesium vapor magnetic system (Scintrex CS-2) was used to collect data at a rate of 10 samples per second. A base station CS-2 was used to diurnally correct the airborne gathered data (Bowslaugh, 2006).

2012 Aurora Silver Mines Limited:
Aurora contracted Canadian Exploration Services (CXS) to conduct a prospecting, ground-based magnetic, and VLF surveys on the Anvil project, which is located near Darby Lake and Morin Lake (Ploeger, 2012a, b). The prospecting survey consisted

of a 500 m-long traverse, aimed at locating historic mine workings and understanding the general geology of the project. Observed rocks were all Nipissing Diabase, and previously unknown shafts and sumps were discovered and their coordinated were recorded with a GPS (Ploeger, 2012a). The geophysics surveys comprised four northwest-oriented lines up to 400 m long and spaced ~75 m apart. Magnetometer and VLF readings were taken every 12.5 meters on the cut lines. The survey outlined the known Nipissing Diabase in the north part of the property (Ploeger, 2012b).

2.5 REGIONAL & LOCAL GEOLOGY

REGIONAL GEOLOGY

The White Reserve project area occurs within the Superior Province, composed of northeast-trending Paleo- to Neoarchean gneissic complexes, granite-greenstone terranes, and sedimentary basins that were assembled by repeated island arc-microcontinent collisions (Bauer et al., 2011). The White Reserve project is partially hosted in Paleoproterozoic (2.5-2.2 Ga) metasedimentary rocks of the Huronian Supergroup (HS) that form a ~60,000 km^2 irregular-shaped siliciclastic paleo-basin, commonly referred to as the Cobalt Embayment (Potter and Taylor, 2009). The metasediments unconformably overly complexly folded and subvertically dipping Neoarchean volcanic, intrusive, and sedimentary rocks of the Wawa-Abitibi terrane that forms the southernmost subprovince of the Canadian portion of the Superior Province (Stott et al., 2010; Stott, 2011; Lodge, 2013). Throughout the region, both the Archean rocks and the HS have been intruded by Nipissing Diabase at approximately 2.219 Ga. These intrusions are primarily tholeiitic, sourced from MORB-type parental magmas, which took advantage of reactivated pre-HS faults (Corfu and Andrews, 1986; Potter and Taylor, 2009). The Nipissing diabase sills are considered the primary heat source that drove hydrothermal fluid circulation resulting in the significant Ag-Co mineralization that occurs throughout the Cobalt Embayment. Figure 4 demonstrates the regional geology including the White Reserve property.
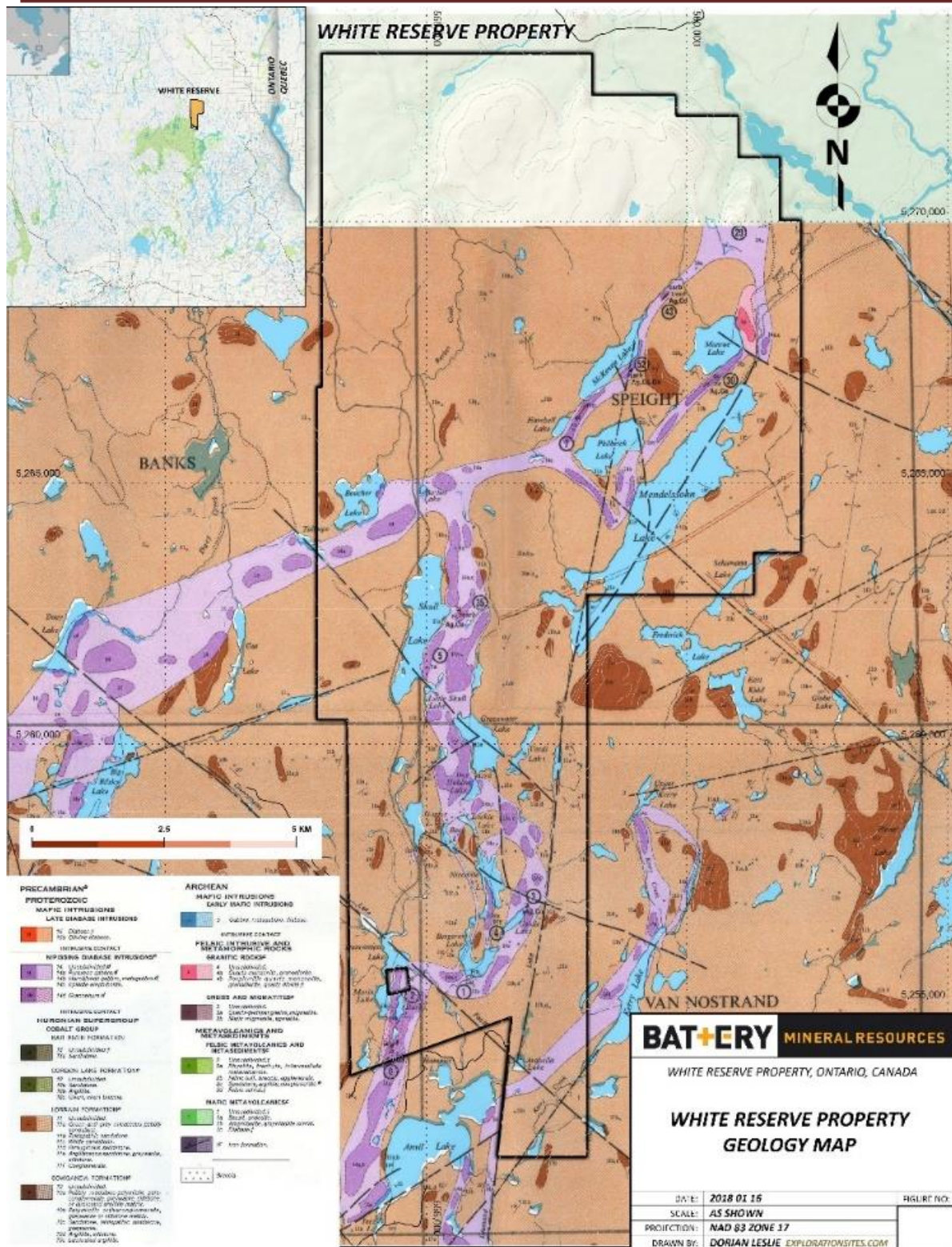
Figure 4: Regional Geology Map including the White Reserve Property.

PROPERTY GEOLOGY

The White Reserve project is dominated by a 150-m-thick, approximately N-S striking Nipissing diabase sill, which intruded Lorraine formation (quartzite or sandstone), part of the Huronian Supergroup (Wilson, 1970). Many silver-cobalt-bearing veins, oriented WNW to EW, occur within the diabase at the surface and underground (George, 1968). There is also a major NW-SE striking fault cutting through the northern part of the property.

2.6 MINERALIZATION

At surface access to mineralization is limited. However, based on the report by George (1968), in which he had underground access, mineralization in the area occurs within vein-filled fractures, ranging from hairline fractures to a maximum width of 3 inches. The dominant sulphide minerals are niccolite and smaltite, with minor amounts of native bismuth and silver. Additionally, disseminated silver mineralization was noted up to 1.5 meters on either side of vein fractures (George, 1968).

3. REFERENCES

Battery Mineral Resources, 2016, Purchase Agreement between Ashley Gold Mines Ltd. and Battery Mineral Resources Ltd. for the Purchase of the White Reserve Claims, Ontario: Battery Mineral Resources Legal Document, 23 p.

Bauer, R.L., Czeck, D.M., Hudleston, P.J., and Tikoff, B., 2011, Structural geology of the subprovince boundaries in the Archean Superior Province of northern Minnesota and adjacent Ontario. In: Miller, J.D., Hudak, G.J., Wittkop, C., McLaughlin, P.I. (Eds.), Archean to Anthropocene: Field Guides to the Geology of the Mid-Continent of North America: Geological Society of America Field Guide 24, p. 203–241.

Bleeker, W., 2015, Synorogenic gold mineralization in granite-greenstone terranes: the deep connection between extension, major faults, synorogenic clastic basins, magmatism, thrust inversion, and long-term preservation, In: Targeted Geoscience Initiative 4: Contributions to the Understanding of Precambrian Lode Gold Deposits and Implications for Exploration, (ed.) B. Dubé and P. Mercier-Langevin; Geological Survey of Canada, Open File 7852, p. 24–47.

Bowslaugh, E., 2006, Midas High Resolution Magnetic Geophysical Survey for Temex Resources Corp., Cobalt Area, Ontario: Fugro Airborne Surveys Report #06003, 38 p.

Bray, J.G., and Geological Staff, 1966, Shatter cones at Sudbury: Journal of Geology, v. 74, p. 243–245.

Castlebar Silver and Cobalt, 1971, Speight Township Report No.11 on Drill Hole SK-1: Ontario Ministry of Northern Development and Mines Assesment Report, 6 p.

Corfu, F., and Andrews, A.J., 1986, A U-Pb age for mineralized Nipissing diabase, Gowganda, Ontario: Canadian Journal of Earth Sciences, v. 23, p.107–109.

Dietz, R.S., 1964, Sudbury structure as an astrobleme: Journal of Geology, v.72, p. 412–434.

Dietz, R.S., and Butler, L.W., 1964, Shatter-cones orientation at Sudbury,Canada: Nature, v. 204, p. 280–281.

French, B.M., 1968, Sudbury structure, Ontario: Some petrographic evidence for an origin by meteorite impact, *in* French, B.M., and Short, N.M., eds., Shock metamorphism of natural materials: Baltimore, Mono Book Corp., p. 383–412.

George, P.T., 1968, Report on the Exploration of the White Reserve Property: Prepared for Argentum Silver Mines, 87 p.

Lodge, R.W.D., 2013, Regional volcanogenic massive sulphide metallogeny of the Neoarchean greenstone belt assemblages of the northwestern margin of the Wawa subprovince, Superior Province: Doctoral dissertation, Laurentian University, Sudbury, Ontario.

Long, G., 2005, Contact Diamond Corperation Report on Ground Geophysics on the Klock Property covering Auld, Barber, Klock, Speigh, and Van Nostrand Townships, Larder Lake Mining Division, Northeastern Ontario: Ontario Ministry of Northern Development and Mines Assessment Report, 70 p.

Mercier-Langevin, P., Gibson, H.L., Hannington, M.D., Goutier, J., Monecke, T., Dubé, B. and Houlé, M.G., 2014, A special issue on Archean magmatism, volcanism, and ore deposits: part 2. Volcanogenic massive sulfide deposits preface: Economic Geology, v. 109(1), p.1-9.

Mortimer, C., 1999, Van Nostrand Property Prospecting Program: Ontario Ministry of Northern Development and Mines Assessment Report, 26 p.

Ploeger, J., 2012a Prospecting Survey over the Anvil Property, Van Nostrand Township, Ontario: Canadian Exploration Services Ltd. Report for Aurora Silver Mines Ltd., 13 p.

Ploeger, J., 2012b Magnetometer and VLF EM Surveys over the Anvil Property, Van Nostrand Township, Ontario: Canadian Exploration Services Ltd. Report for Aurora Silver Mines Ltd., 16 p.

Potter, E.G. and Taylor, R.P., 2009, The lead isotope composition of ore minerals from precious metal-bearing, polymetallic vein systems in the Cobalt Embayment, northern Ontario: metallogenetic implications: Economic Geology, v. 104(6), p.869-879.

Rungis, A.C., 2008, Prospecting Survey Anvil Property, Van Nostrand Township, Ontario: Klondike Silver Corp. Report, 18 p.

Schuur, W., 1969, Report on Airborne Magnetic Survey in the Anvil Lake area, Ontario: Canadian Aero Mineral Surveys report for Union Miniere Exploration and Mining Corporation Limited, 12 p.

Stanwick, S., 1971, Speight Township Report No.10 on Drill Hole SK-1: Ontario Ministry of Northern Development and Mines Assessment Report, 3 p.

Stott, G.M., 2011, A Revised Terrane Subdivision of the Superior Province of Ontario: Ontario Geological Survey, Miscellaneous Release – Data, 278 p.

Stott, G.M., Corkery, M.T., Percival, J.A., Simard, M., and Goutier, J., 2010, A revised terrane subdivision of the Superior Province. In: Summary of Field Work and Other Activities, Open File Report 6260: Ontario Geological Survey, pp. 20–21 to 20–10.

Therriault, A.M., Fowler, A.D., and Grieve, R.A., 2002, The Sudbury Igneous Complex: A differentiated impact melt sheet: Economic Geology, v. 97(7), p.1521-1540.

Walker, R.J., Morgan, J.W., Naldrett, A.J., Li, C. and Fassett, J.D., 1991, Re-Os isotope systematics of Ni-Cu sulfide ores, Sudbury Igneous Complex, Ontario: evidence for a major crustal component: Earth and Planetary Science Letters, v. 105(4), p.416-429

Wilson, B., 1970, Report on a soil geochemical sampling program in Speight Township, Ontario, Canada. Ontario Ministry of Northern Development and Mines Assesment Report, 11 p.

Young, G.M., Long, D.G., Fedo, C.M., and Nesbitt, H.W., 2001, Paleoproterozoic Huronian basin: product of a Wilson cycle punctuated by glaciations and a meteorite impact: Sedimentary Geology, v. 141, p. 233-254.

4. QUALIFICATIONS

STATEMENT OF QUALIFICATIONS

I, C. Jason Ploeger, hereby declare that:

1. I am a professional geophysicist with residence in Larder Lake, Ontario and am presently employed as a Geophysicist and Geophysical Manager of Canadian Exploration Services Ltd. of Larder Lake, Ontario.

2. I am a Practicing Member of the Association of Professional Geoscientists, with membership number 2172.

3. I graduated with a Bachelor of Science degree in geophysics from the University of Western Ontario, in London Ontario, in 1999.

4. I have practiced my profession continuously since graduation in Africa, Bulgaria, Canada, Mexico and Mongolia.

5. I am a member of the Ontario Prospectors Association, a Director of the Northern Prospectors Association and a member of the Society of Exploration Geophysicists.

6. I do not have nor expect an interest in the properties and securities of **Battery Mineral Resources Ltd.**

7. I am responsible for the compilation of the presentation of this report. The statements made in this report represent my professional opinion based on my consideration of the information available to me at the time of writing this report.

C. Jason Ploeger, P.Geo., B.Sc.
Geophysical Manager
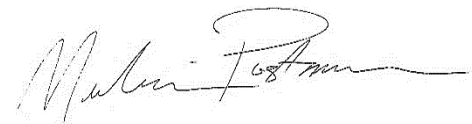Canadian Exploration Services Ltd.

Larder Lake, ON
November 25, 2019

CERTIFICATE OF QUALIFICATION AND CONSENT

STATEMENT OF QUALIFICATIONS

I, Melanie Postman, hereby declare that:

1. I am a Geoscientist-in-Training with residence in Larder Lake, Ontario and am presently employed as a Junior Geophysicist with Canadian Exploration Services Ltd. of Larder Lake, Ontario.

2. I graduated with a Bachelor of Science Honors specialization degree in geophysics for professional registration from the University of Western Ontario, in London Ontario, in 2017.

3. I am a member of the Association of Professional Geoscientists as a Geoscientist-in-Training (Member ID 10710).

4. I have previous geophysical work experience during and following my education.

5. I do not have nor expect an interest in the properties and securities of **Battery Mineral Resources Ltd.**

6. I am responsible for assisting with the final processing and validation of the survey results and the compilation of the presentation of this report. The statements made in this report represent my opinion based on my consideration of the information available to me at the time of writing this report.

Melanie Postman, GIT, B.Sc.
Junior Geophysicist

Larder Lake, ON
November 25, 2019

CERTIFICATE OF QUALIFICATION AND CONSENT

I, Frank Rainer Ploeger of the town of Virginiatown, Province of Ontario, do hereby certify:

1) That I am a Consulting Geologist and reside at 21 Waite Avenue, Virginiatown, Ontario, P0K 1X0.

2) That I graduated from Queen's University at Kingston, Ontario with a Bachelor of Applied Science degree in 1973; and, that I completed 2 years of an MSc program at McMaster University in Hamilton, Ontario (1980- 1982).

3) That I am a **member in good standing of the Association of Geoscientists of Ontario (#479), the Association of Professional Engineers and Geoscientists of Saskatchewan (#10852, non- practicing), the Geological Association of Canada, the Prospectors and Developers Association, and the Northern Prospectors Association**. I have received a temporary permit (#2153) to practice in Quebec from the Ordre des geologues du Quebec pending acceptance by the Office quebequois de la langue francaise (OQLF).

4) That I have practiced my profession as a mineral exploration and mine geologist for a period of about 45 years.

5) This document is based on information various public documents and my personal observations during several visits to the property.

Although the information supplied to me is believed to be accurate and all reasonable care has been taken in the completion of this report, I hereby disclaim any and all liability arising out of its use and circulation. While I stand behind my interpretations, I cannot guarantee the accuracy of the source information and the use of this report or any part thereof shall be at the user's sole risk.

6) I have no interest, either directly or indirectly, in the subject property or client company.

7) *My written permission is required for the release of any summary or excerpt.*

_____

Frank R. Ploeger   Virginiatown, Ontario, Nov 25, 2019

APPENDIX I

Precision GeoSurveys Report

Precision
GeoSurveys

AIRBORNE GEOPHYSICAL SURVEY REPORT

White Reserve Survey Block
Gowganda, Ontario
Battery Mineral Resources Pty. Ltd.

Precision GeoSurveys Inc.
www.precisiongeosurveys.com
Hangar 42 Langley Airport
21330 - 56th Ave., Langley, BC
Canada V2Y 0E5
604-484-9402

Jenny Poon, B.Sc., P.Geo.
Shawn Walker, M.Sc., P.Geo.
October 2018
Job# 18122-WR

Table of Contents

List of Figures

Precision
GeoSurveys

List of Tables

List of Appendices

Appendix A: Equipment Specifications
Appendix B: Digital File Descriptions

List of 2016 and 2018 White Reserve Blocks Plates (Scale 1:45,000)

Plate 1: 2016 and 2018 White Reserve - Actual Flight Lines (FL)
Plate 2: 2016 and 2018 White Reserve - Digital Terrain Model (DTM)
Plate 3: 2016 and 2018 White Reserve - Total Magnetic Intensity with Actual Flight Lines (TMI_wFL)
Plate 4: 2016 and 2018 White Reserve - Total Magnetic Intensity (TMI)
Plate 5: 2016 and 2018 White Reserve - Residual Magnetic Intensity (RMI)
Plate 6: 2016 and 2018 White Reserve - Calculated Vertical Gradient (CVG) of RMI
Plate 7: 2016 and 2018 White Reserve - Reduced to Magnetic Pole (RTP) of RMI
Plate 8: 2016 and 2018 White Reserve - First Vertical Derivative (1VD) of RTP
Plate 9: 2016 and 2018 White Reserve - Calculated Horizontal Gradient (CHG) of RMI
Plate 10: 2016 and 2018 White Reserve - Potassium – Percentage (%K)
Plate 11: 2016 and 2018 White Reserve - Thorium – Equivalent Concentration (eTh)
Plate 12: 2016 and 2018 White Reserve - Uranium – Equivalent Concentration (eU)
Plate 13: 2016 and 2018 White Reserve - Total Count (TC)
Plate 14: 2016 and 2018 White Reserve - Total Count – Exposure Rate (TCexp)
Plate 15: 2016 and 2018 White Reserve - Potassium over Thorium Ratio (%K/eTh)
Plate 16: 2016 and 2018 White Reserve - Potassium over Uranium Ratio (%K/eU)
Plate 17: 2016 and 2018 White Reserve - Uranium over Thorium Ratio (eU/eTh)
Plate 18: 2016 and 2018 White Reserve - Uranium over Potassium Ratio (eU/%K)
Plate 19: 2016 and 2018 White Reserve - Thorium over Potassium Ratio (eTh/%K)
Plate 20: 2016 and 2018 White Reserve - Thorium over Uranium Ratio (eTh/eU)
Plate 21: 2016 and 2018 White Reserve - Ternary Map (TM)

Precision
GeoSurveys

1.0 <u>Introduction</u>

This report outlines the geophysical survey operations and data processing procedures taken during the high resolution helicopter-borne aeromagnetic and radiometric survey flown over the 2018 White Reserve survey block for Battery Mineral Resources Pty. Ltd. The 2018 survey block is located northeast of Sudbury (Figure 1) in northeastern Ontario, bordering the northern edge of a survey block flown in 2016. The geophysical survey was flown on July 11, 2018 and July 14, 2018.
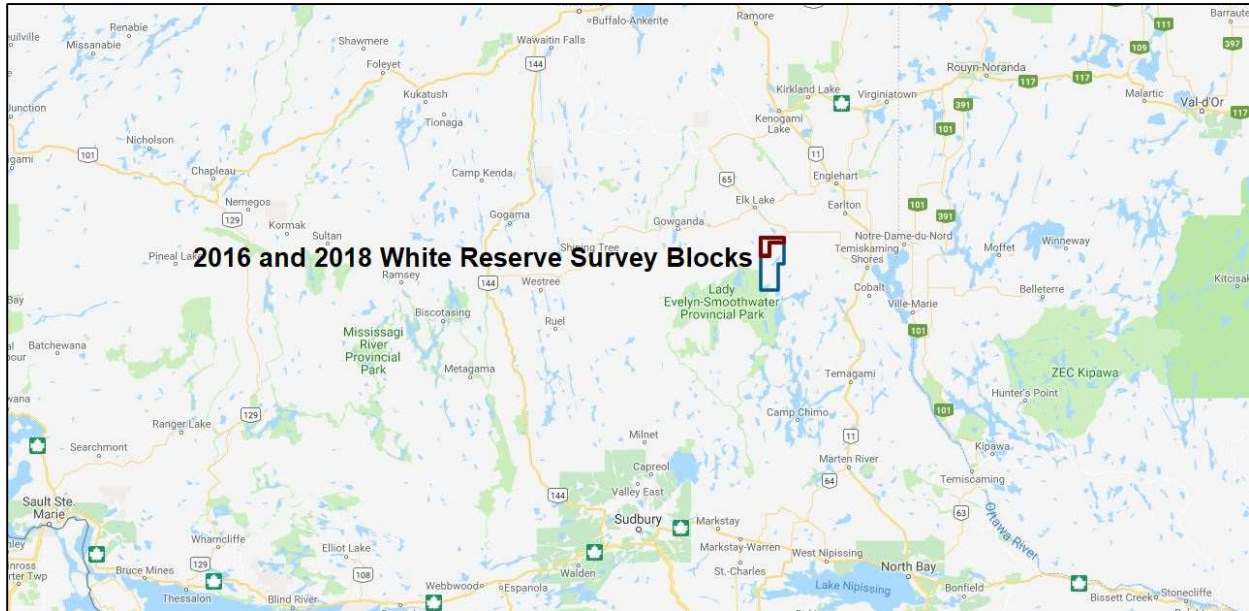
Figure 1: 2016 White Reserve – Speight (blue) and 2018 White Reserve (red) survey blocks location map.

1.1 Survey Area

The 2018 White Reserve survey block covers a total area of 42.2 km^2, centered approximately 135 km northeast of Sudbury, Ontario and 25 km east of Gowganda, Ontario (Figure 2).
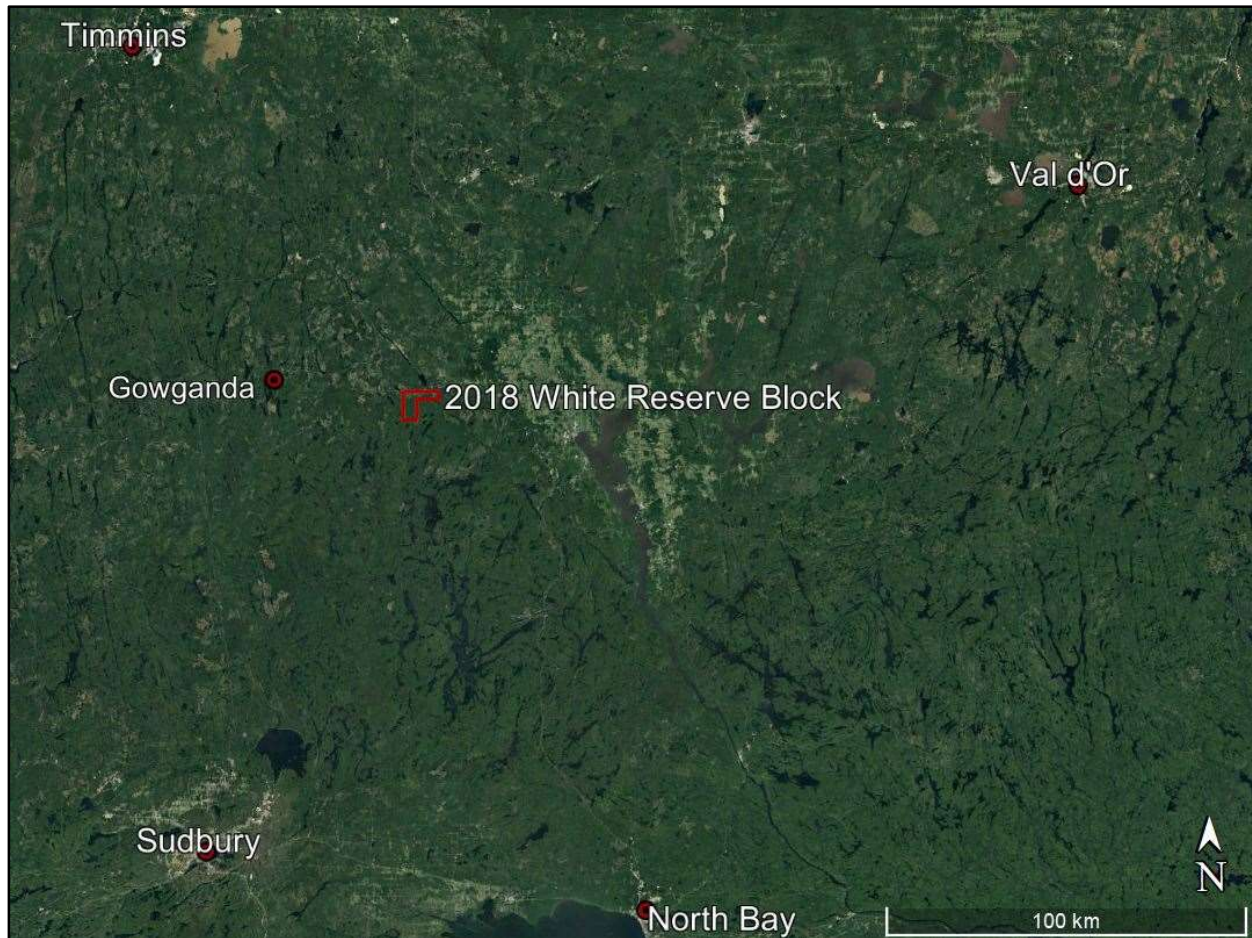
Figure 2: 2018 White Reserve survey block shown in red 135 km northeast of Sudbury, Ontario.

A total of 464 line km of magnetic and radiometric data was collected on 100 survey lines and 8 tie lines over the 2018 survey block. The survey was flown at 100 meter spacings at a heading of 000°/180°; tie lines were flown at 1000 meter spacings at a heading of 090°/270° (Figures 3 and 4). The 2018 survey was designed to expand on the magnetic and radiometric survey area flown in 2016, so that a total of 2197 line km of survey data were collected over a total combined area of 195.7 km^2 (Figure 5). The 2018 survey block overlaps a 2.7 km^2 area at the northern margins of the 2016 White Reserve - Speight survey block with 63 duplicated line km for merging and leveling purposes.

Job#18122-WR

Figure 3: Plan View – 2018 White Reserve survey block boundary in red with actual flight lines in yellow.

Figure 4: Terrain View – 2018 White Reserve survey block with actual flight lines displayed in yellow.

3
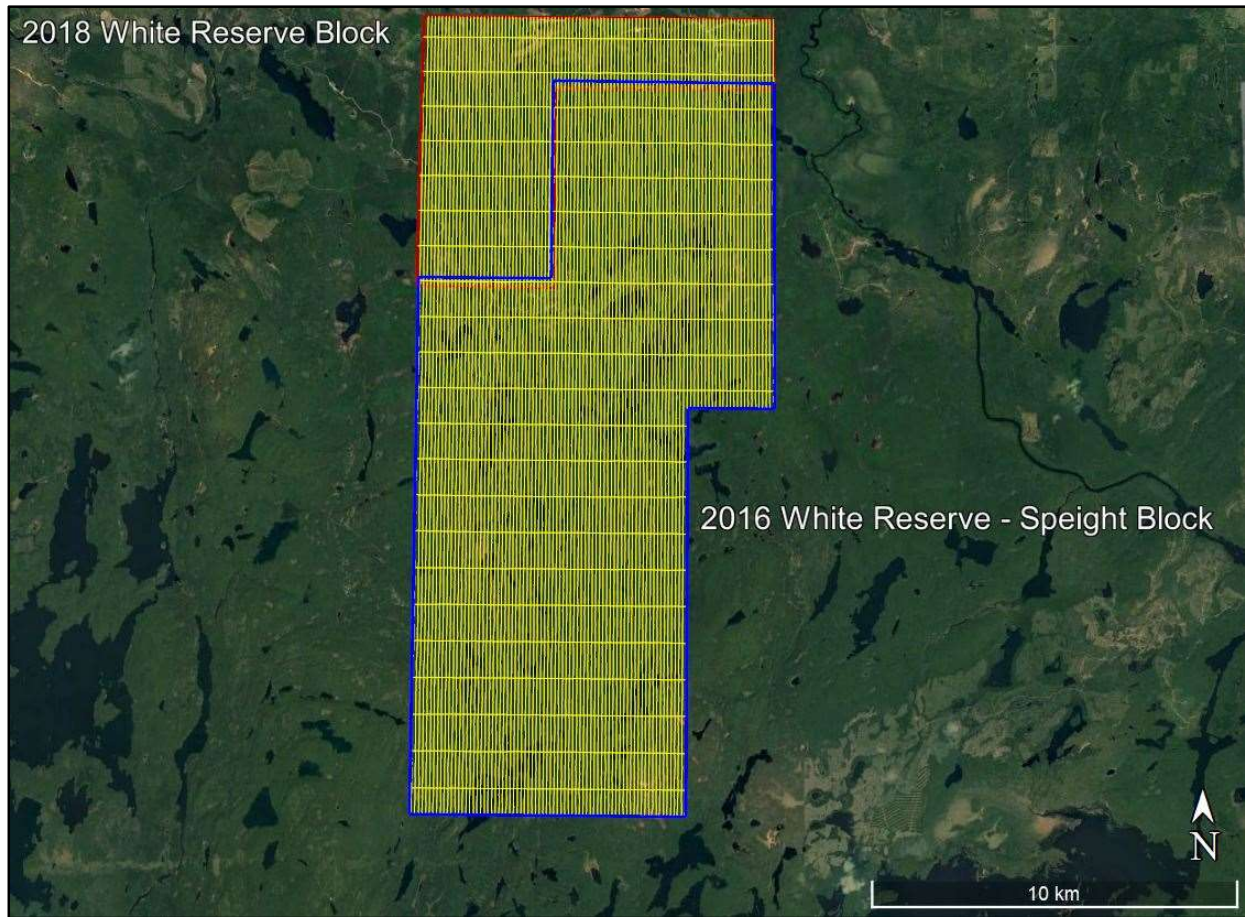
Figure 5: Plan View – Combined 2016 (blue) and 2018 (red) survey blocks at the White Reserve survey area with actual flight lines in yellow. An area of 8.8 km^2 was flown as overlap between the two blocks.

1.2   Survey Specifications

The geodetic system used for the geophysical survey was WGS 84 in UTM Zone 17N. A total of 464 line km was flown over 42.2 km^2 (Table 1). Polygon coordinates for the 2018 survey block are specified in Table 2. The 2018 survey block adjoins the survey block flown in 2016 which covered 156.2 km^2 with 1733 line km of magnetic and radiometric data.

Survey Block	Area (km²)	Line Type	No. of Lines Planned	No. of Lines Completed	Line Spacing (m)	Line Orientation (UTM grid)	Actual Survey Height (m)	Total Planned Line km	Total Actual km Flown
2018 White Reserve	42.2	Survey	100	100	100	000°/180°	38.8	421	421
		Tie	8	8	1000	090°/270°	42.5	43	43
		Total:	**108**	**108**				**464**	**464**
2016 White Reserve - Speight	156.2	Survey	100	100	100	000°/180°	39.4	1569	1578
		Tie	20	20	1000	090°/270°	40.2	154	155
		Total:	**120**	**120**				**1723**	**1733**
2016-2018 White Reserve (combined)	195.7	Survey	200	200	100	000°/180°	39.0	1990	1999
		Tie	28	28	1000	090°/270°	41.3	197	198
		Total:	**228**	**228**				**2187**	**2197**

Table 1: 2016 and 2018 White Reserve – survey flight line specifications. A total of 63 line km were duplicated over a 2.7 km² overlap area. Refer to 2016 report for additional details.

Longitude (deg)	Latitude (deg)	Easting (m)	Northing (m)	N/S	E/W
80.29883686	47.61745045	552689	5274021	N	W
80.16659755	47.61668292	562627	5274034	N	W
80.16688750	47.59842830	562627	5272005	N	W
80.24914941	47.59862736	556443	5271964	N	W
80.24915307	47.54721322	556498	5266250	N	W
80.30068190	47.54790792	552620	5266291	N	W

Table 2: 2018 White Reserve survey boundary polygon coordinates using WGS 84 in UTM Zone 17N.

2.0 <u>Geophysical Data</u>

Geophysical data are collected in a variety of ways and are used to aid in determination of geology, mineral deposits, oil and gas deposits, geotechnical investigations, contaminated land sites, and UXO (unexploded ordnance) detection.

For the purposes of this survey, airborne magnetic and radiometric data were collected to serve in geological mapping and exploration for mineral deposits.

2.1 Magnetic Data

Magnetic surveying is the most common airborne geophysical technology used for both mineral and hydrocarbon exploration. Aeromagnetic surveys measure and record the total intensity of the magnetic field at the magnetometer sensor, which is a combination of the desired magnetic field generated in the Earth as well as small variations due to the temporal effects of the

constantly varying solar wind and the magnetic field of the survey aircraft. By subtracting the temporal, regional, and aircraft effects, the resulting aeromagnetic map shows the spatial distribution and relative abundance of magnetic minerals - most commonly the iron oxide mineral magnetite - in the upper levels of Earth's crust, which in turn are related to lithology, structure, and alteration of bedrock. Survey specifications, instrumentation, and interpretation procedures depend on the objectives of the survey. Magnetic surveys are typically performed for:

- Geological Mapping - to aid in mapping lithology, structure, and alteration.

- Depth to Basement Mapping - for exploration in sedimentary basins or mineralization associated with the basement surface.

2.2   Radiometric Data

Radiometric surveys are used to determine either the absolute or relative amounts of uranium (U), thorium (Th), and potassium (K) in surface rocks and soils using natural radioactive emanations. Gamma radiation is utilized due to its greater penetration depth compared with alpha and beta radiation. Radiometric data are useful for mapping lithology, alteration, and structure as well as providing insights into weathering. For example, the natural radioactivity of igneous rocks generally increases with SiO_2 content and clay minerals tend to fix the natural radioelements.

Gamma rays are electromagnetic waves with frequencies between 10^{19} and 10^{21} Hz emitted spontaneously from an atomic nucleus during radioactive decay, in packets referred to as photons. The energy E transported by a photon is related to the wavelength λ or frequency ν by the formula:

$$E = h\nu = hc/\lambda$$

        where: c is the velocity of light
                    h is Planck's constant (6.626 x 10^{-34} joule).

All detectable gamma radiation from Earth materials comes from the natural decay products of three primary radioelements: U, Th, and K. Each individual nuclear species (isotope) emits gamma rays at one or more specific energies, as shown in Figure 6. Of the three main natural radioactive elements, only potassium (^{40}K) emits gamma energy directly, at 1.46 MeV. Uranium (^{238}U) and thorium (^{232}Th) emit gamma rays through their respective decay series; ^{214}Bi at 1.76 MeV for uranium and ^{208}Tl at 2.61 MeV for thorium. Accordingly, the ^{214}Bi and ^{208}Tl measurements are considered equivalents for uranium (eU) and thorium (eTh), as the daughter products will be in equilibrium under most natural conditions.
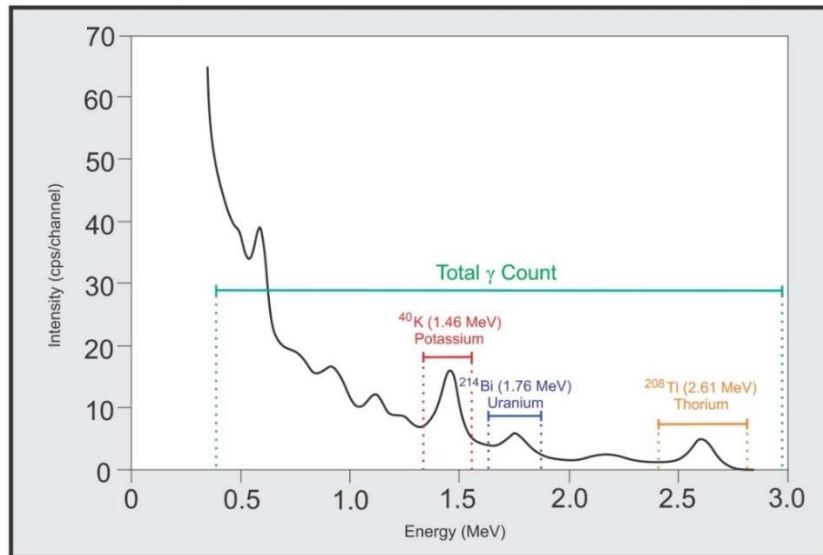
Figure 6: Typical natural gamma spectrum showing the three spectral windows (^{40}K 1.37-1.57 MeV, ^{214}Bi 1.66-1.86 MeV, ^{208}Tl 2.41-2.81 MeV) and total count (0.40-2.81 MeV) window.

Surficial debris, vegetation, standing water (lakes, marshes, swamps), and snow can effectively attenuate gamma rays originating from underlying rocks. Therefore, variations in isotope counts must be evaluated with respect to surficial conditions before they are attributed to changes in underlying geology. An increase in soil moisture can also significantly affect gamma radiation concentrations. For example, a 10% increase in soil moisture can decrease the measured gamma radiation by about the same amount. Radon isotopes are long-lived members of both the U and Th decay series and Ra mobility can influence radiometric surveys. In addition to being directly radioactive, ^{226}Ra and ^{222}Rn can attach to dust particles in the atmosphere. Radioactive precipitation of these dust particles by rain can lead to apparent increases of more than 2000% in uranium ground concentration (IAEA, 2003). Therefore, gamma ray surveying should not be carried out during a rainfall, or shortly after a rainfall.

3.0   <u>Survey Operations</u>

The geophysical survey was flown on July 11, 2018 and July 14, 2018 in dry weather conditions. The experience of the pilot ensured that the data quality objectives were met, and that the safety of the flight crew was never compromised given the potential risks involved in airborne geophysical surveying. Field processing and quality control checks were performed daily.

3.1   **Operations Base and Crew**

The base of operations was in Gowganda, Ontario (Figure 7) west of the 2018 White Reserve survey block.
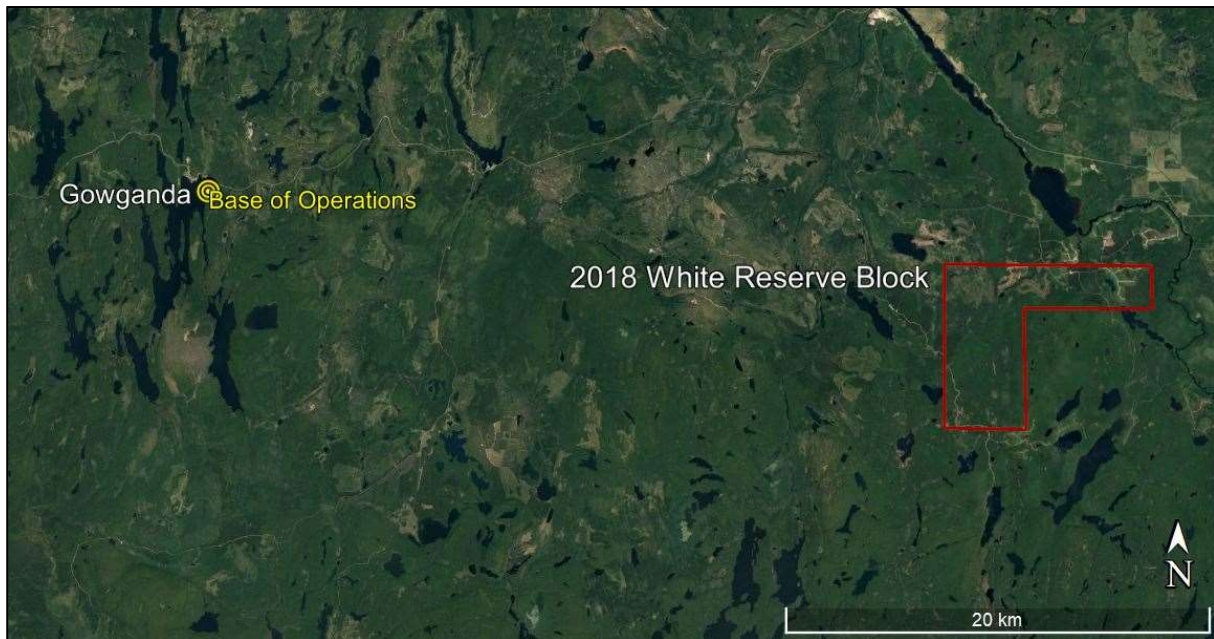
Figure 7: Map showing base of operations in Gowganda, Ontario west of the 2018 White Reserve survey block.

The Precision geophysical crew consisted of five members (Table 3):

Crew Member	Position
Don Plattel	Helicopter survey pilot
Jonathan Passiniemi	Geophysical operator and electronics technician (on-site)
Jenny Poon, B.Sc., P.Geo.	Geophysicist and data processor (off-site)
Shawn Walker, M.Sc., P.Geo.	Geophysicist and data processor (off-site)
Collin Paul, B.Sc.	Geophysicist – reporting and mapping

Table 3: List of survey crew members.

3.2   Magnetic Base Station Specifications

Changes in the Earth's magnetic field over time, such as diurnal variations, magnetic pulsations, and geomagnetic storms, were measured and recorded by two GEM GSM-19T proton precession magnetometers. The magnetic base stations were installed in an area (Table 4; Figures 8 and 9) of low magnetic noise away from metallic items such as ferromagnetic objects, vehicles, or power lines that could affect the base stations and ultimately the survey data.

Station name	Easting/Northing	Longitude/Latitude	Datum/ Projection
GEM 5 S/N 1094678	0517441E, 5277009N	80° 46' 03.99" W 47° 38' 46.48" N	WGS 84, Zone 17N
GEM 6 S/N 5087249	0517438E, 5276996N	80° 46' 04.14" W 47° 38' 46.06" N	WGS 84, Zone 17N

Table 4: Magnetic base station locations.

8

Magnetic readings were reviewed at regular intervals to ensure that no airborne data were collected during periods of high magnetic activity (greater than 10 nT change per minute).
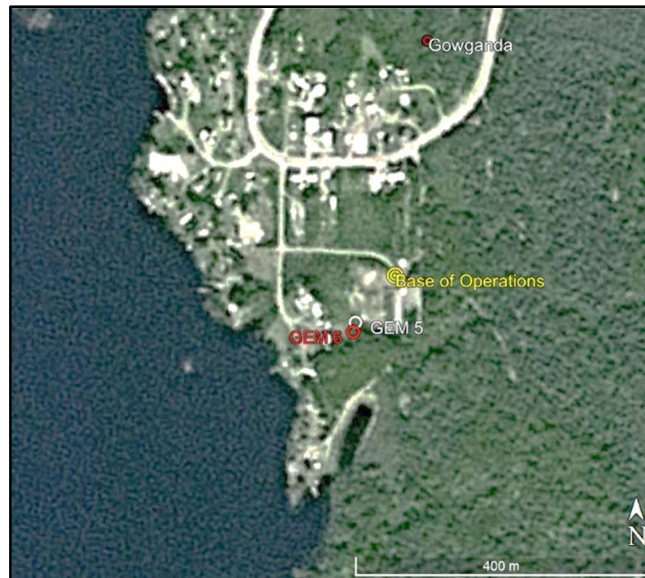
Figure 8: GEM 5 and GEM 6 magnetic base stations located at the Gowganda Motel.

Figure 9: GEM 5 (left) and GEM 6 (right) magnetic base stations located in a field behind the Gowganda Motel.

3.3   Field Processing and Quality Control

On a flight-by-flight basis, survey data were transferred from the aircraft's data acquisition system onto a USB memory stick and copied onto a field data processing laptop. The raw data files in PEI binary data format were converted into Geosoft GDB database format. Using Geosoft Oasis Montaj 9.4.3, the data were inspected to ensure compliance with contract specifications (Table 5; Figures 10 to 12). A radiometric test line, T10080, was flown every survey day. Two minutes of accumulated gamma data were averaged on a daily basis to monitor the effects of moisture on radiometric data and to observe the behaviour of the gamma-ray spectrometer in the air over time (Figure 13).

Parameter	Specification	Tolerance
Position	Line Spacing	Flight line deviation within 10 m L/R from ideal flight path. No exceedance for more than 1 km.
	Height	Nominal flight height of 35 m AGL with tolerance of +/- 10 m. No exceedance for more than 1 km, provided deviation is not due to tall trees, topography, mitigation of wildlife/livestock harassment, cultural features, or other obstacles beyond the pilot's control.
	GPS	GPS signals from four or more satellites must be received at all times, except where signal loss is due to topography. No exceedance for more than 1 km.
Magnetics	Temporal/Diurnal Variations	Non-linear temporal magnetic variations within 10 nT of a linear chord of length 1 minute.
	Normalized 4th Difference	Magnetic data within 0.05 nT peak to peak. No exceedance for distances greater than 1 km or more, provided noise is not due to geological or cultural features.

Table 5: Contract survey specifications. Specified survey height was intentionally exceeded over cabins.

Precision
GeoSurveys
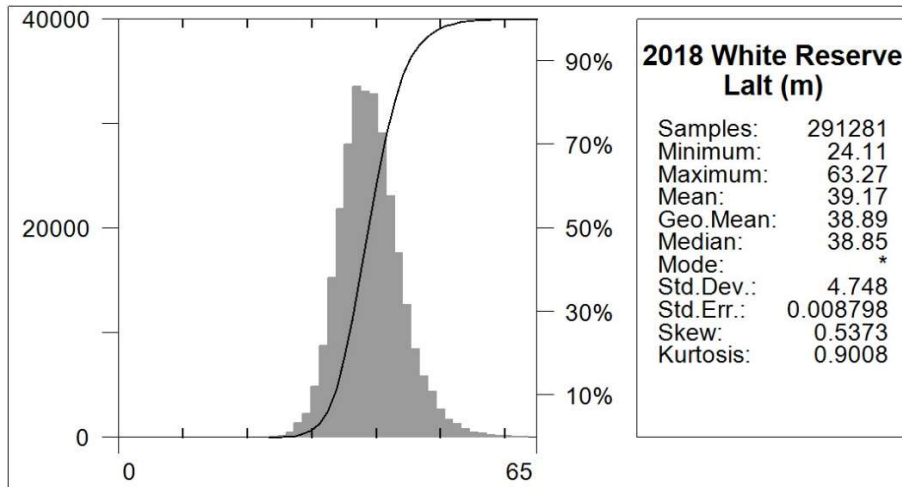
Figure 10: Histogram showing survey elevation vertically above ground. Specified survey height was intentionally exceeded over cabins.
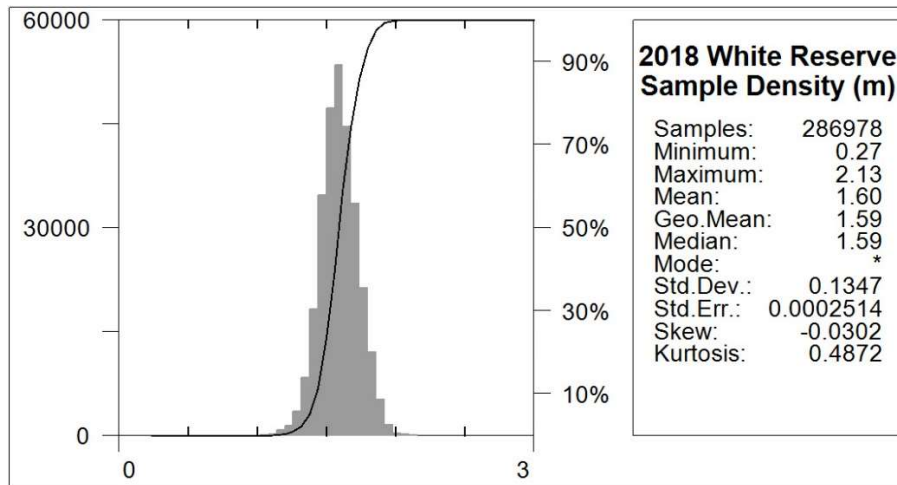
Figure 11: Histogram showing magnetic sample density. Horizontal distance in meters between adjacent measurement locations; magnetic sample frequency 20 Hz.
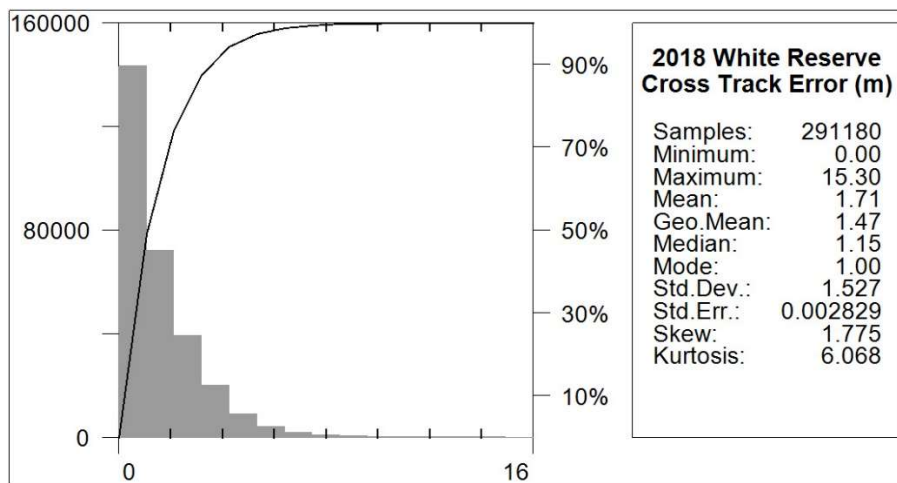
Figure 12: Histogram showing cross track error.

11
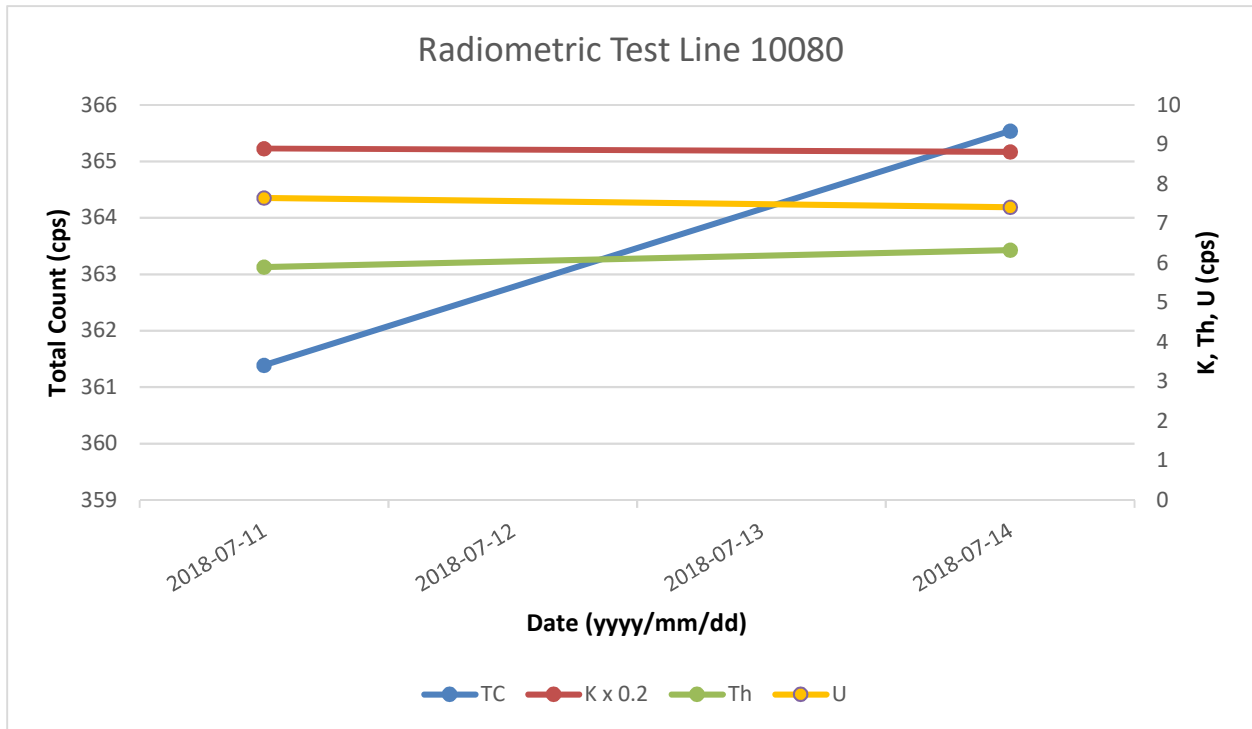
Figure 13: Radiometric test line – Tie Line 10080 flown once each survey day. Average counts of TC, K, Th, and U data. No survey flights were flown at White Reserve on July 12th and 13th. The maximum daily variance was 2% over the entire survey period.

4.0   Aircraft and Equipment

All geophysical and subsidiary equipment were carefully installed on a Precision GeoSurveys aircraft to collect integrated magnetic and radiometric data.

4.1   Aircraft

Precision GeoSurveys flew the survey using a Bell 206B Jet Ranger helicopter, registration C-FZHK, at a nominal height of 35 m AGL.

4.2   Geophysical Equipment

The survey aircraft (Figure 14) was equipped with a magnetometer, spectrometer, data acquisition system, laser altimeter, magnetic compensation system, barometer, temperature/humidity probe, pilot guidance unit (PGU), and GPS navigation system. In addition, two magnetic base stations were used to record temporal magnetic variations.

Figure 14: Survey helicopter equipped with geophysical equipment.

4.2.1 AGIS

The Airborne Geophysical Information System (AGIS), manufactured by Nuvia - Pico Envirotec, is the main computer used in integrated data recording, data synchronizing, displaying real-time quality control data for the geophysical operator and the generation of navigation information for the pilot and operator display systems. Information such as magnetic field components, aircraft position, survey altitude, and survey speed are recorded to solid-state memory and can all be monitored on the AGIS airborne operator's display (Figure 15) for immediate quality control.

Figure 15: AGIS operator display installed in the Bell 206B Jet Ranger survey helicopter, with screen displaying real time flight line recording and navigation parameters. Additional windows display real time geophysical data to operator.

13

4.2.2 Magnetometer

A Scintrex CS-3 cesium vapor magnetometer (S/N 0706248) is a high sensitivity/low noise magnetometer with automatic hemisphere switching and a wide voltage range; the static noise rating for the unit is +/- 0.01 nT. Total magnetic field data were recorded at 20 Hz. A separate fluxgate magnetometer determined the aircraft's attitude (pitches, rolls, and yaws) relative to the inclination and declination of the Earth's magnetic field, which was necessary to remove magnetic noise created by movement of the aircraft through a compensation process. The magnetic sensors were mounted on the front of the helicopter in an approved non-magnetic and non-conductive "stinger" configuration (Figure 16) to reduce influence from the aircraft's magnetic field.

Figure 16: View of cesium vapor magnetometer. Sensor oriented 45° from vertical to couple with local magnetic field at the White Reserve survey block.

14

Precision
GeoSurveys

4.2.3 Spectrometer

The GRS-10 radiometric data acquisition system is a fully integrated gamma radiation detection system (Figure 17) containing a total of 8.4 litres of downward-looking NaI(Tl) synthetic crystals, with 256 channel output at 1 Hz sampling rate. The two downward-looking crystals are designed to measure gamma rays from below the aircraft and are installed in the rear cabin of the helicopter.

Figure 17: GRS-10 thallium-activated sodium iodide gamma spectrometer crystal packs. The open unit on the right shows two individual 4.2 litre gamma detectors.

4.2.4 Magnetic Base Station

To monitor and record the Earth's temporal magnetic field variations, particularly diurnal, Precision GeoSurveys operated two GEM GSM-19T base station magnetometers at all times while airborne data were being collected. The base stations were located in an area with low magnetic gradient, away from electric power transmission lines and moving ferrous objects, such as motor vehicles, that could affect the survey data integrity.

The GEM GSM-19T magnetometer (Figure 18) with integrated GPS time synchronization uses proton precession technology with a 1 Hz sampling rate. The GSM-19T has an absolute accuracy of +/- 0.2 nT and sensitivity of 0.15 nT at 1 Hz. Base station magnetic data were recorded on internal solid-state memory and downloaded onto a field laptop computer using a serial cable and GEMLink 5.4 software. Profile plots of the base station readings were generated, updated, and reviewed at the end of each survey day.

Figure 18: GEM GSM-19T proton precession magnetometer.

4.2.5 Laser Altimeter

Terrain clearance is measured by an Opti-Logic RS800 Rangefinder laser altimeter (Figure 19) attached to the aft end of the magnetometer boom. The RS800 laser is a time-of-flight sensor that measures distance by a rapidly modulated and collimated laser beam that creates a dot on the target surface. The maximum range of the laser altimeter is 700 m off natural surfaces with an accuracy of +/- 1 meter on 1 x 1 m diffuse target with 50% (+/- 20%) reflectivity. Within the sensor unit, reflected signal light is collected by the lens and focused onto a photodiode. Through serial communications and digital outputs, ground clearance data are transmitted to an RS-232 compatible port and recorded and displayed by the AGIS and PGU at 10 Hz in meters.
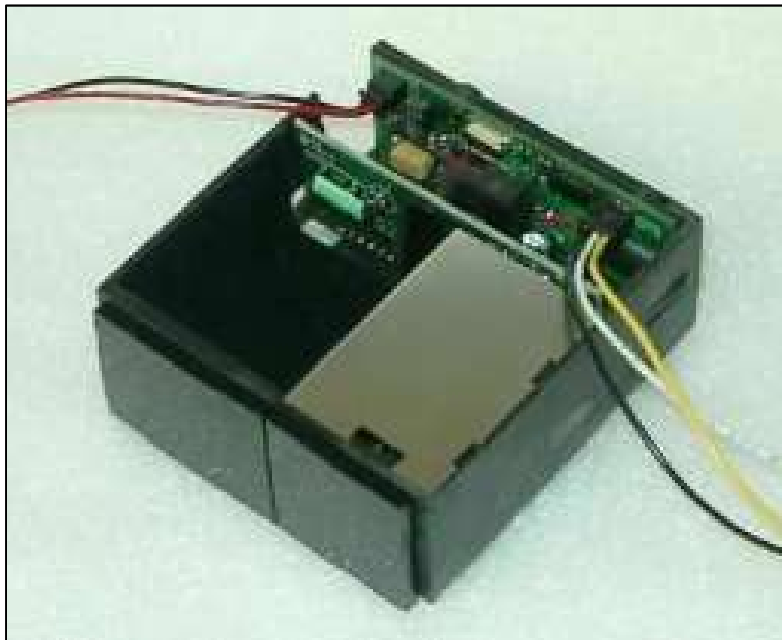
Figure 19: Opti-Logic RS800 Rangefinder laser altimeter.

4.2.6 Pilot Guidance Unit

Steering and elevation (ground clearance) information is continuously provided to the pilot by the Pilot Guidance Unit (PGU). The graphical display is mounted on top of the aircraft's instrument panel, remotely from the data acquisition system. The PGU is the primary navigation aid (Figure 20) to assist the pilot in keeping the aircraft on the planned flight path, heading, speed, and at the desired ground clearance.
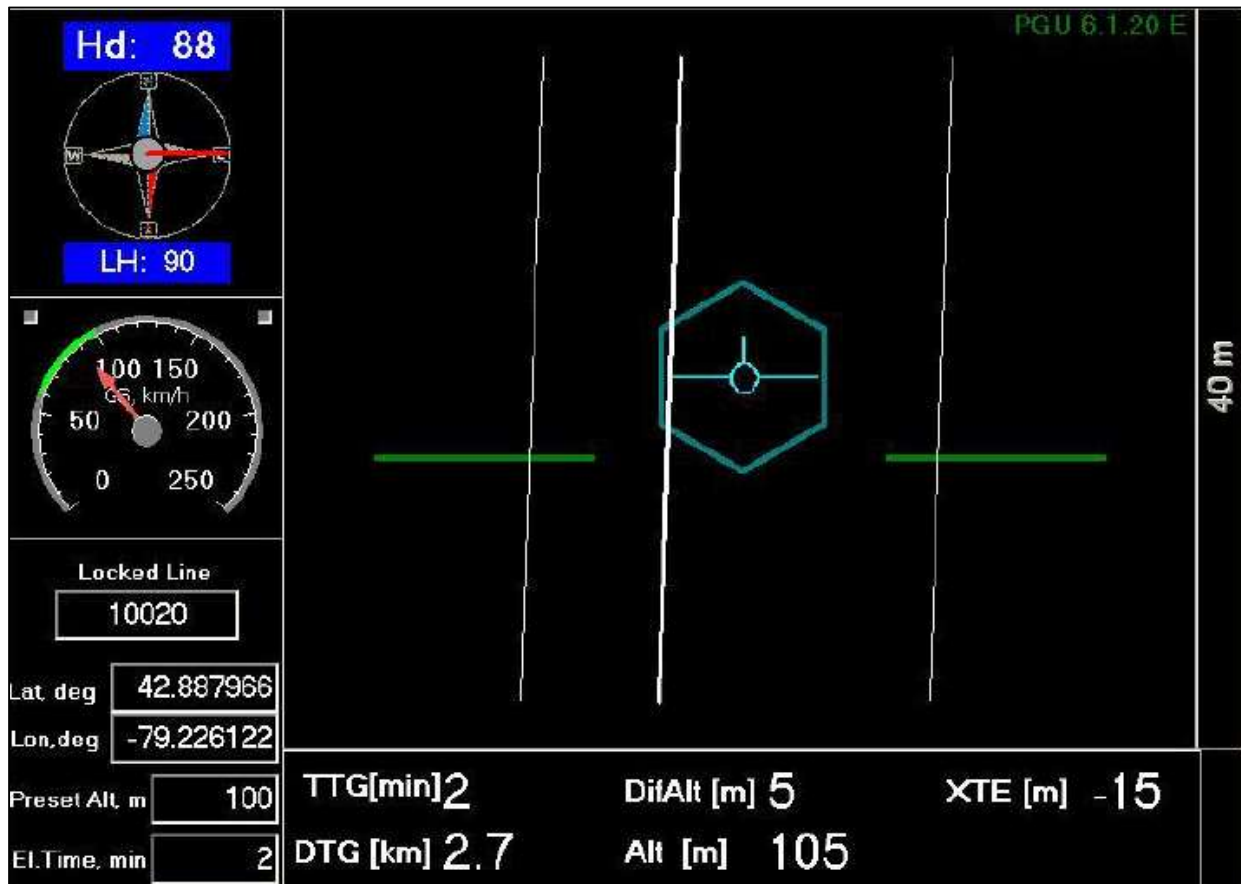
Figure 20: PGU screen displaying navigation information.

The LCD monitor is a full VGA 800 x 600 pixel 7 inch (17.8 cm) display. The CPU for the PGU is contained in a PC-104 console and uses Microsoft Windows operating system control, with input from the GPS antenna, embedded drape surface profile or laser altimeter, and AGIS.

4.2.7 GPS Navigation System

A Hemisphere R220 GPS receiver (Figure 21) and a Novatel GPS antenna integrated with the AGIS navigation system and pilot display (PGU) to provide accurate navigational information and control. The R220 GPS receiver supports fast updates and outputs messages at a rate of up to

20 Hz (20 times per second); delivering sub-meter positioning accuracy in three dimensions. It supports GNSS (GPS/GLONASS) L1 and L2 signals.

The receiver supports differential correction methods including L-Band, RTK, SBAS and Beacon. The R220 employs innovative Hemisphere GPS Eclipse SureTrack technology, which allows it to model the phase on satellites that the airborne unit is currently tracking. With the SureTrack technology, dropouts are reduced and the speed of the signal reacquisitions is increased; enhancing accurate positioning when base corrections are not available.

Figure 21: Hemisphere R220 GPS receiver.

5.0   Data Acquisition Equipment Checks and Calibration

Airborne equipment tests and calibrations were conducted for the laser altimeter, magnetometer, and spectrometer. A lag test was performed for all three sensors. There were two tests conducted for the airborne magnetometer: compensation flight and heading error test. There were three tests conducted for the gamma spectrometer: calibration pad test, cosmic flight test, and altitude correction and sensitivity test.

5.1   Lag Test

A lag test was performed to determine the difference in time the digital reading was recorded for the magnetometer, gamma spectrometer, and laser altimeter with the position fix time that the

fiducial of the reading was obtained by the GPS system resulting from a combination of system lag and different locations of the various sensors and the GPS antenna. The test was flown in the four orthogonal survey headings over an identifiable magnetic anomaly at survey speed and height. The resulting data (Table 6) were used to correct for time and position.

Sensor	Fiducials	Seconds
Magnetometer	6	0.30
Spectrometer	7	0.35
Laser altimeter	8	0.40

Table 6*: Survey lag corrections.*

5.2   Magnetometer Tests

The magnetometer was tested and calibrated with a series of dedicated flights specifically for removing undesired effects of aircraft movement, speed, and heading direction.

5.2.1 Compensation Flight Test

During aeromagnetic surveying a small but significant amount of noise is introduced to the magnetic data by the aircraft itself, as the magnetometer is within the aircraft's magnetic field. Movement of the aircraft (roll, pitch, and yaw) combined with the permanent magnetization of certain aircraft parts (in particular the engine and other ferrous magnetic objects) contribute to this noise. The aircraft was degaussed using proprietary technology prior to starting the survey and the remaining magnetic noise was removed by a process called magnetic compensation.

A magnetic compensation flight was completed (Table 7). The process consists of a series of prescribed maneuvers where the aircraft flies in the four orthogonal headings required for the survey (000°/090°/180°/270° in the case of this survey) at a sufficient altitude (typically > 2,500 m AGL) in an area of low magnetic gradient where the Earth's magnetic field becomes nearly uniform at the scale of the compensation flight. In each heading direction, three specified roll, pitch, and yaw maneuvers (total 36) are performed by the pilot at constant elevation so that any magnetic variation recorded by the airborne magnetometer can be attributed to aircraft movement. These maneuvers are recorded by the airborne fluxgate magnetometer and provide the data that are required to calculate the necessary parameters for compensating the magnetic data to remove aircraft noise from survey data.

Pre-Compensation					Post-Compensation				
Heading	Roll	Pitch	Yaw	Total	Heading	Roll	Pitch	Yaw	Total
000°	0.7480	0.5466	0.3084	1.6030	000°	0.0754	0.1109	0.0802	0.2665
090°	0.6132	0.4580	0.2482	1.3194	090°	0.0772	0.0801	0.0894	0.2467
180°	0.7063	0.2345	0.3068	1.2476	180°	0.0420	0.0505	0.0638	0.1563
270°	0.5795	0.4491	0.2771	1.3057	270°	0.0608	0.0751	0.0642	0.2001
Total	2.6470	1.6882	1.1405		Total	0.2554	0.3166	0.2976	
FOM (nT) = 5.4757					FOM (nT) = 0.8696				

Table 7: Figure of Merit maneuver test results for 000°/090°/180°/270° compensation flight flown on June 25, 2018.

5.2.2 Heading Error Test

To determine the magnetic heading effect a cloverleaf pattern flight test was conducted. The cloverleaf test was flown in the same orthogonal headings (Table 8) as the survey and tie lines (000°/090°/180°/270°) at >1000 m AGL in an area with low magnetic gradient. For the cloverleaf test, the survey aircraft must pass over the same mid-point all four times at the same elevation so that any change in measured magnetic intensity can be attributed to heading.

Heading	Fiducial	Mag (nT)	Correction (nT)
000°	2086.50	55536.74	0.80
090°	1302.45	55536.85	0.70
180°	1684.00	55538.80	-1.25
270°	1102.90	55537.80	-0.25
	Average	55337.55	
	Total		0.00

Table 8: Heading error test data format flown on June 25, 2018.

5.3   Gamma-ray Spectrometer Tests and Calibrations

Calibration and testing of the GRS-10 airborne gamma-ray spectrometry system was carried out prior to the start of the survey. The calibration of the spectrometer system involved three tests which enabled the conversion of airborne data to ground concentration of natural radioactive elements. These tests were the calibration pad test, cosmic flight test, and the altitude correction and sensitivity test. Measurements were made in accordance with IAEA technical report series No. 323, *Airborne Gamma Ray Spectrometer Surveying*, and AGSO Record 1995/60, *A Guide to the Technical Specifications for Airborne Gamma-Ray Surveys*.

Precision
GeoSurveys

5.3.1 Calibration Pad Test

The calibration pad test was conducted by Pico Envirotec using GSC (Geological Survey of Canada) portable calibration pads. The pads are slabs of concrete containing known concentrations of the radioelements (K, Th, and U) and are used to simulate ideal geological sources of radiation. The measurements collected from the calibration pad test were used to determine the Compton scattering and Grasty backscatter (spectral overlap between element windows) coefficients.

5.3.2 Cosmic Flight Test

While the background source of gamma radiation from the aircraft itself is essentially constant, the amount of signal detected from ground sources varies with ground clearance. As the height of the aircraft increases, the distance between the ground and the spectrometer crystals increases, and the proportion of cosmic radiation in each spectral window increases exponentially due to radiation of cosmic origin. The cosmic flight test is conducted to determine the aircraft's background attenuation coefficients for the detector crystal packs and the cosmic coefficients. The pilot is required to fly over the same location repeatedly in opposite directions at the following elevations in meters above ground; 900, 1500, 2100, 2400, and 2700, for approximately 2 minutes each to collect gamma data used to determine the amount of non-terrestrial gamma signal.

5.3.3 Altitude Correction and Sensitivity Test

The altitude and sensitivity test is similar to the cosmic flight test but is conducted at lower elevations (from ground level). The pilot is required to fly over the same location at the following elevations in meters above ground; 30, 60, 90, 120, 150, 210, 270 and 360, for 2 minutes each. As the distance of the aircraft increases above the radioactive ground source, the source signature exponentially degrades. As a result, this test is used to determine the altitude attenuation coefficients and the radio-element sensitivity of the airborne spectrometer system.

6.0 <u>Data Processing</u>

After all data were collected, several procedures were undertaken to ensure that the data met a high standard of quality. Data recorded by the AGIS were converted into Geosoft or ASCII file formats by using Pico Envirotec software. Further processing (Figure 22) was carried out using Geosoft Oasis Montaj 9.4.3 geophysical processing software along with proprietary processing algorithms. Radiometric, laser, and GPS data were resampled to 20 Hz to correspond with the magnetic sample rate.
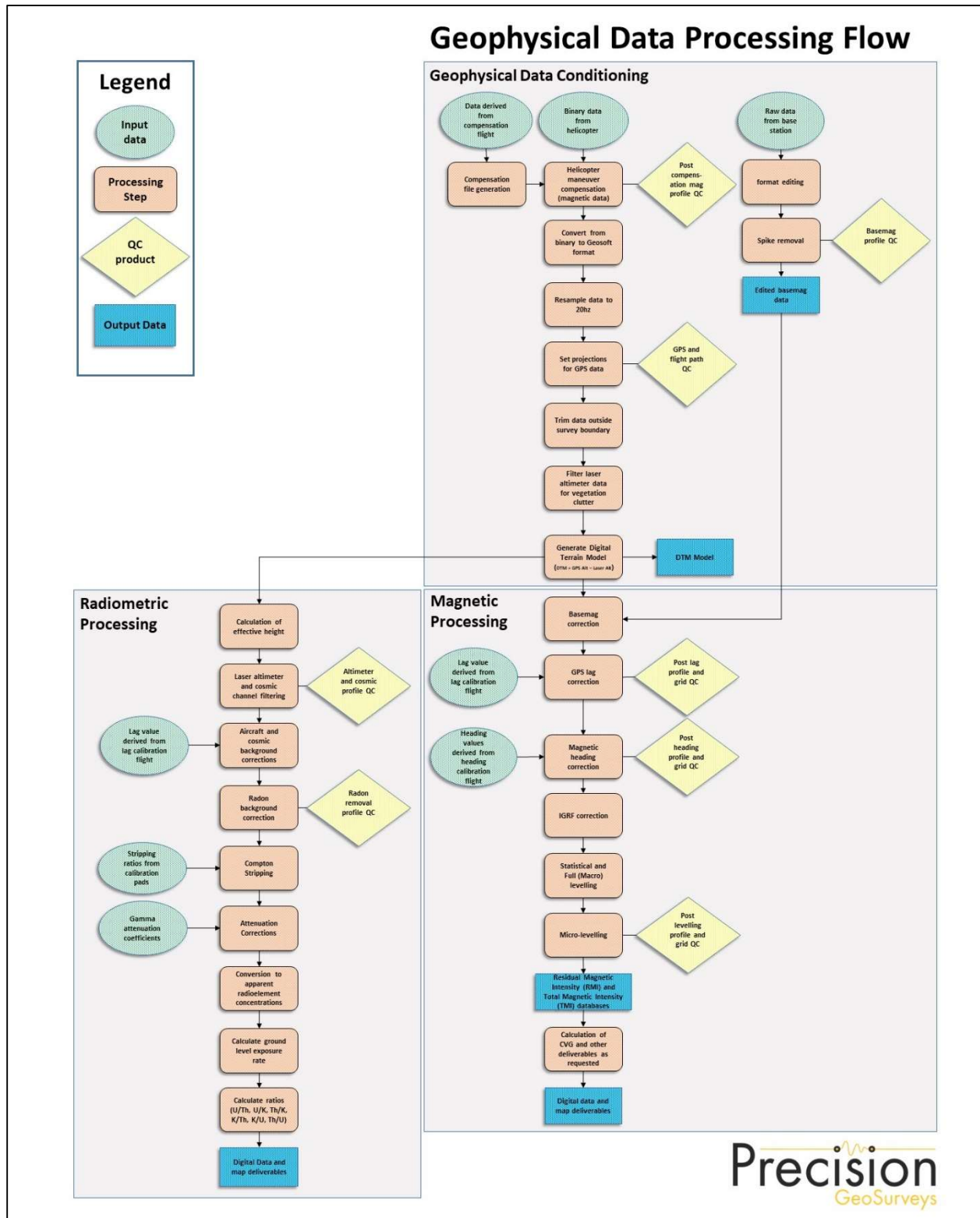
Figure 22: Magnetic and radiometric data processing flow.

6.1   Flight Height and Digital Terrain Model

Laser altimeters cannot provide valid data over glassy water, fog, or dense vegetation. Over areas with dense vegetation a certain proportion of the laser signal does not penetrate through the trees to record actual ground clearance and high frequency variations are recorded. A Rolling Statistics filter was applied to the lag-corrected laser altimeter data to remove vegetation clutter. A Low Pass filter was then applied to smooth out the laser altimeter profile to eliminate isolated high frequency noise and generate a surface closely corresponding to the actual ground profile.

A Digital Terrain Model (DTM) channel was calculated by subtracting the processed laser altimeter data from the filtered GPS altimeter data defined by the WGS 84 ellipsoidal height. DTM accuracy is affected by the geometric relationship between the GPS antenna and the laser altimeter as well as flight attitude of the aircraft, slope of the ground, and sample density.

6.2   Magnetic Processing

Raw magnetic data, as collected by the airborne instruments, were corrected for aircraft influence, flight maneuvers, temporal variations, lag, and heading. The data were examined for magnetic noise and spikes, which were removed as required. Survey and tie line data of the resulting total magnetic field were leveled and the background magnetic field, International Geomagnetic Reference Field of the Earth, removed.

6.2.1   Flight Compensation

Data obtained from the compensation flight test were applied to the raw magnetic data as the first step of data processing. A computer program called PEIComp was used to create a model from the compensation flight test for each survey to remove the noise induced by the aircraft and its movement; this model was applied to data from each survey flight.

6.2.2   Base Station Correction

The next step in processing the compensated magnetic data was to correct for temporal variation of the Earth's magnetic field. Magnetic data from base station GEM 6 were used for correcting the airborne magnetic survey data, and GEM 5 data were retained for backup. The data were edited, plotted, and merged into a Geosoft database (.GDB) on a daily basis.

The base station measurements were averaged to establish a magnetic reference datum at 55457.93 nT, and this value was used to calculate the observed magnetic base station deviations resulting from variations of the Earth's magnetic field over time with reference to the datum. The airborne magnetic data were then corrected for temporal variations by subtracting the base

station deviations from the data collected on the aircraft, which effectively removed the effects of diurnal and other temporal variations.

6.2.3 Lag Correction

Following the base station correction, a lag correction of 0.3 seconds was applied to each total magnetic field data point to compensate for the combination of lag in the recording system and the magnetometer sensor flying 14.7 m ahead of the GPS antenna.

6.2.4 Heading Correction

For each survey heading, changes in instrument magnetic fields along a survey flight line are detected and these systematic shifts are recorded. These values are used to construct a heading table (.TBL) file. An intersection table was created, containing all magnetic field values where tie lines intersected the survey lines and the overall average magnetic field value was calculated. For each of the four headings, the averages were calculated and then compared to the overall average to determine four values to be used for heading error correction in each flight direction.

6.2.5 IGRF Removal

The International Geomagnetic Reference Field (IGRF) model is the empirical representation of the Earth's magnetic field (main core field without external sources) collected and disseminated from satellite data and from magnetic observatories around the world. The IGRF is generally revised and updated every five years by a group of modelers associated with the International Association of Geomagnetism and Aeronomy (IAGA). Accordingly, the 12th generation IGRF (IGRF-12), an IGRF model for epoch 2015.0 was used with the actual survey date obtained from the "Date" channel.

Residual Magnetic Intensity (RMI) was calculated by taking the difference between IGRF and the non-leveled Total Magnetic Intensity (TMI). This created a more valid model of individual near-surface anomalies so that the data were not referenced to a specific time. This will allow for other magnetic data (historic or future) to be more easily incorporated into each survey database.

6.2.6 Leveling and Micro-leveling

Residual Magnetic Intensity (RMI) data from survey and tie lines were used to level the entire survey dataset. Two types of leveling were applied to the corrected data: conventional leveling and micro-leveling. There were two components to conventional leveling; statistical leveling to level tie lines and full leveling to level survey lines. The statistical leveling method corrected the SL/TL intersection errors that follow a specific pattern or trend. Through the error channel, an algorithm calculated a least-squares trend line and derived a trend error curve, which was then

added to the channel to be leveled. The second component was full leveling. This adjusted the magnetic value of the survey lines so that all lines matched the trended tie lines at each intersection point.

Following statistical leveling, micro-leveling was applied to the corrected conventional leveled data. This iterative grid-based process removed low amplitude components of flight line noise that still remained in the data after tie line and survey line leveling and resulted in fully leveled RMI data. The IGRF was then added back onto the RMI to allow for the production of a leveled TMI grid and map.

6.2.7 Reduction to Magnetic Pole

Reduced to Magnetic Pole (RTP) data were computed from the leveled Residual Magnetic Intensity (RMI) data. The RTP filter was applied in the Fourier domain and it migrates the observed magnetic inclination and declination field to what the field would look like at the north magnetic pole.

6.2.8 Calculation of First Vertical Derivative

The first vertical derivatives were computed from both the leveled Residual Magnetic Intensity (RMI) data and the Reduced to Magnetic Pole (RTP). The first vertical derivative calculates the vertical rate of change in the magnetic field. It is used to enhance shorter wavelength signals; therefore, edges of magnetic anomalies are highlighted, and deep geologic sources in the data are suppressed.

The first vertical derivative calculated from the RMI was designated as Calculated Vertical Derivative of RMI, or CVG. The first vertical derivative calculated from the RTP was designated as First Vertical Derivative of RTP, or 1VD.

Vertical derivative to the nth derivative is:

$$L(r) = r^n$$

6.2.9 Calculation of Horizontal Gradient

The Calculated Horizontal Gradient (CHG) is the magnitude of the total horizontal gradient. It is used to estimate contact locations of magnetic bodies at shallow depths, reveal anomaly texture, and highlight anomaly-pattern discontinuities.

If M is the magnetic field, then the CHG is calculated as:

$$\text{CHG}(x, y) = \sqrt{\left(\frac{\partial M}{\partial x}\right)^2 + \left(\frac{\partial M}{\partial y}\right)^2}$$

6.3   Radiometric Processing

Radiometric surveys map gamma rays from the concentration of radioelements at or near Earth's surface; typically, up to 1.5 meters below surface. Before any processing of the airborne radiometric data, the spectrometer system is calibrated with the calibration pad test, cosmic flight test, and altitude correction and sensitivity test. Once calibration of the system was complete, the radiometric data were processed by windowing the full spectrum to create individual channels for U, Th, K, and total count.

Steps taken to process acquired radiometric data are summarized below:

- Calculation of effective height
- Lag Correction
- Aircraft and Cosmic background corrections
- Radon background correction
- Stripping ratios
- Attenuation corrections
- Conversion to apparent radioelement concentrations

6.3.1   Calculation of Effective Height

Laser/Radar altimeter data were converted to effective height (h_{ef}) in meters using the acquired laser/radar altimeter, temperature and pressure data, according to the formula below:

$$h_{ef} = h * \frac{273.15}{T + 273.15} * \frac{P}{1013.25}$$

where: h is observed laser/radar altitude in meters

T is measured air temperature in degrees Celsius

P is barometric pressure in millibars

6.3.2   Lag Correction

Following the calculation of effective height, a lag correction of 0.35 seconds was applied to each radiometric channel to compensate for the combination of lag in the recording system and the difference in position of the spectrometer and the GPS antenna.

26

Precision
GeoSurveys

6.3.3 Aircraft and Cosmic Background Corrections

Aircraft background and cosmic stripping corrections are applied to all three elements, and total count, using the following formula:

$$C_{ac} = a_c + b_c * Cos_f$$

> where: C_{ac} is the background and cosmic corrected channel
> a_c is the aircraft background for this channel
> b_c is the cosmic stripping coefficient for this channel
> Cos_f is the filtered cosmic channel

6.3.4 Radon Background Correction

To strip the effects of atmospheric radon from the downward-looking detectors, there are multiple methods available for radon background estimation. The method selected was the background table method. Procedures to the background table method and how to determine the radiometric values filled within the table in detail are outlined in the IAEA 1363 report, *Guidelines for Radioelement Mapping using Gamma Ray Spectrometry Data*.

6.3.5 Compton Stripping

Spectral overlap corrections are applied to potassium, uranium, and thorium as part of the Compton stripping process. This is done by using the stripping ratios that have been calculated for the spectrometer by prior calibration; this breaks the corrected elemental values down into the apparent radioelement concentrations.

Stripping ratios α, β, and γ are first modified according to altitude. Then an adjustment factor (derived from the cosmic flight test), the reversed stripping ratio, uranium into thorium, is calculated.

$$\alpha_h = \alpha + h_{ef} * 0.00049$$

$$\beta_h = \beta + h_{ef} * 0.00065$$

$$\gamma_h = \gamma + h_{ef} * 0.00069$$

> where: $\alpha, \beta. \gamma$ are the Compton stripping coefficients
> $\alpha_h, \beta_h. \gamma_h$ are the height corrected Compton stripping coefficients
> h_{ef} is the effective height above ground in metres at STP

Precision
GeoSurveys

The stripping corrections are then carried out using the following formulas:

$$Th_c = Th_{bc}(1 - g\beta_h) + U_{bc}(b\gamma_h - a) + K_{bc}(ag - b)/A$$

$$U_c = Th_{bc}(g\beta_h - \alpha_h) + U_{bc}(1 - b\beta_h) + K_{bc}(b\alpha_h - g)/A$$

$$K_c = [Th_{bc}(\alpha_h\gamma_h - \beta_h) + U_{bc}(a\beta_h - \gamma_h) + K_{bc}(1 - a\alpha_h)]/A$$

  where: U_c, Th_c, and K_c are stripping corrected uranium, thorium and potassium
     $\alpha_h, \beta_h. \gamma_h$ are height corrected Compton stripping coefficients
     U_{bc}, Th_{bc}, and K_{bc} are background corrected uranium, thorium and potassium
     a is the spectral ratio Th/U
     b is the spectral ratio Th/K
     g is the spectral ratio U/K
     $A = 1 - g\gamma_h - (\alpha_h - g\beta_h) - b(\beta_h - \alpha_h\gamma_h)$ is the backscatter correction

6.3.6 Attenuation Corrections

The total count, potassium, uranium, and thorium data are then corrected to a nominal survey altitude (corrected to remove vegetation clutter from radar/laser altimeter data), in this case the survey height was 35 meters. This is done according to the equation:

$$C_a = C * e^{\mu(h_{ef} - h_0)}$$

  where: C_a is the output altitude corrected channel
     C is the input channel
     μ is the attenuation correction for that channel
     h_{ef} is the effective altitude, usually in m
     h_0 is the nominal survey altitude used as datum

6.3.7 Conversion to Apparent Radioelement Concentrations

With all corrections applied to the radiometric data, the final step is to convert the corrected potassium ([40]K), uranium (from [214]Bi), and thorium (from [212]Tl) to apparent radioelement concentrations using the following formula:

$$eE = C_{cor}/S$$

  where: eE is the element concentration K (%) and equivalent element concentration
     of U (ppm) & Th (ppm)
     S is the experimentally determined sensitivity
     C_{cor} is the fully corrected channel

Precision
GeoSurveys

Conversion of total count to natural exposure rate (Grasty et al, 1984) is determined by using the following formula:

$$\text{Natural Exposure} = [(1.505 * K) + (0.625 * eU) + (0.31 * eTh)]$$

where: Natural Exposure in µR/hr
K is the concentration of potassium (%)
eU is the equivalent concentration of uranium (ppm)
eTh is the equivalent concentration of thorium (ppm)

6.3.8 Radiometric Ratios

To calculate some of the common radiometric ratios (U/Th, Th/K, and U/K and their inverses) the guidelines of the IAEA are followed. Due to statistical uncertainties in the individual radioelement measurements, care is taken during ratio calculation in order to obtain statistically significant values. The following guidelines were used to determine the ratios:

1. For each concentration the lowest corrected count rate is determined.
2. Element concentrations of adjacent points on either side of each data point are summed until they exceed a pre-determined threshold value.
3. The ratios are calculated using the accumulated sums.

With these guidelines, errors associated with the calculated ratios are minimized and comparable for all data points.

6.3.9 Ternary Radioelement Map

A ternary radioelement map is an image which maps each of the primary colours, yellow, magenta, and cyan, in proportion to the radioelement concentration values of the K, Th, and U grids. Areas of low radioactivity, and consequently low signal to noise ratios, can be masked and are shaded in white by setting the TC as the shaded grid.

6.4 Merging 2016 and 2018 Data

Magnetic and radiometric data collected from the 2016 survey were merged and leveled to the survey data collected in 2018. This was accomplished by performing statistical leveling using 2016 tie lines and 2018 survey lines.

Magnetic data collected where the survey and tie lines intersected help determine leveling values to be applied to level the 2016 data to 2018 data to produce a complete leveled RMI grid. Subsequently, to merge 2016 and 2018 TMI data, a 2018 date was used to recalculate a new IGRF which was then added back onto the RMI to produce a merged and leveled TMI grid and

map. The date that was used to recalculate the IGRF was July 14, 2018; the last full day of surveying at the 2018 White Reserve survey block.

Using a similar method to merge the radiometric data, common lines flown in 2016 and 2018 were compared and the differences were used to determine average leveling constants. These values were applied to 2018 data and then merged with 2016 data to produce complete leveled radiometric grids.

7.0 Deliverables

Survey data are presented as digital databases, maps, and a logistics report.

7.1 Digital Data

The digital files have been provided in two formats, the first is a .GDB file for use in Geosoft Oasis Montaj and the second format is a text (.XYZ) file. Full descriptions of the digital data and contents are included in the report (Appendix B).

The digital data were represented as grids as listed below:

- Digital Terrain Model (DTM)
- Total Magnetic Intensity (TMI)
- Residual Magnetic Intensity (RMI) – removal of IGRF from TMI
- Calculated Vertical Gradient (CVG) – first vertical derivative of RMI
- Reduced to Magnetic Pole (RTP) – reduced to magnetic pole of RMI
- First Vertical Derivative (1VD) – first vertical derivative of RTP
- Calculated Horizontal Gradient (CHG) – total horizontal gradient of RMI
- Potassium – Percentage (%K)
- Thorium – Equivalent Concentration (eTh)
- Uranium – Equivalent Concentration (eU)
- Total Count (TC)
- Total Count – Exposure Rate (TCexp)
- Potassium over Thorium Ratio (%K/eTh)
- Potassium over Uranium Ratio (%K/eU)
- Uranium over Thorium Ratio (eU/eTh)
- Uranium over Potassium Ratio (eU/%K)
- Thorium over Potassium Ratio (eTh/%K)
- Thorium over Uranium Ratio (eTh/eU)
- Ternary Map (TM)

Precision
GeoSurveys

7.1.1 Grids

2018 and merged 2016 and 2018 digital data were gridded and displayed using the following Geosoft parameters:

- Grid cell size: 25 m
- Low-pass desampling factor: 2
- Tolerance: 0.001
- % pass tolerance: 99.99
- Maximum iterations: 100

All grids were drawn with a histogram-equalized color shade; sun illumination inclination at 45° and declination at 045°.

7.2 KMZ

The digital data represented as grids were exported into .kmz files which can be displayed using Google Earth. The grids can be draped onto topography and rendered to give a 3D view.

7.3 Maps

Digital maps were created for the merged and leveled 2016 and 2018 White Reserve survey blocks. The following map products were prepared:

Overview Maps (colour images with elevation contour lines):

- Actual flight lines, with block boundaries and claim outlines
- DTM

Magnetic Maps (colour images with elevation contour lines):

- TMI with actual flight lines
- TMI
- RMI
- CVG of RMI
- RTP of RMI
- 1VD of RTP
- CHG of RMI

Radiometric Maps (colour images with elevation contour lines):

- %K – Percentage

- eTh – Equivalent Concentration
- eU – Equivalent Concentration
- TC
- TCexp – Exposure Rate
- %K/eTh Ratio
- %K/eU Ratio
- eU/eTh Ratio
- eU/%K Ratio
- eTh/%K Ratio
- eTh/eU Ratio
- Ternary Map

All survey maps were prepared in WGS 84 and UTM Zone 17N.

7.4   Report

A pdf copy of the logistics report is included along with digital data and maps. The report provides information on the data acquisition procedures, data processing, and presentation of the 2016 and 2018 White Reserve survey blocks data.

8.0 <u>Conclusions and Recommendations</u>

The geophysical survey covered areas with multiple potential sources of cultural and magnetic interference, in particular; industrial equipment and cabins. The magnetic and radiometric signals have been affected by both varying flying height and cultural features.

While the objective of geophysical data processing is to accurately represent the Earth's geophysical features, continual processing, such as the calculation of derivatives, can generate false features as the signal-to-noise ratio decreases. In addition, false features can appear near the edges of a survey block where gridding algorithms are unable to properly calculate grids, such as in "edge effects." Therefore, subtle geophysical features in derivative-enhanced map products or near the survey margins must be used with discretion.

The airborne geophysical data were acquired to map the geophysical characteristics of the survey area, which are in turn related to the distribution and concentration of magnetic minerals and radioactive elements in the Earth. Geophysical data are not a direct indication of mineral deposits and therefore interpretation and careful integration with existing and new geological, geochemical, and other geophysical data are recommended to maximize value from the survey investment.

Appendix A
Equipment Specifications

- GEM GSM-19T Proton Precession Magnetometer (Magnetic Base Station)
- Hemisphere R220 GPS Receiver
- Opti-Logic RS800 Rangefinder Laser Altimeter
- Setra Model 276 Barometric Pressure
- Scintrex CS-3 Survey Magnetometer
- Billingsley TFM100G2 Ultra Miniature Triaxial Fluxgate Magnetometer
- Pico Envirotec GRS-10 Gamma Spectrometer
- Pico Envirotec AGIS data recorder system (for navigation and geophysical data acquisition)

GEM GSM-19T Proton Precession Magnetometer (Magnetic Base Station)

Sensitivity	0.15 nT @ 1 Hz
Resolution	0.01 nT (gamma), magnetic field and gradient
Absolute accuracy	± 0.2 nT @ 1 Hz
Operating Range	20,000 to 120,000 nT
Gradient Tolerance	Over 7,000 nT/m
Operating Ranges	Temperature: -40°C to +50°C Battery Voltage: 10.0 V minimum to 15 V maximum Humidity: up to 90% relative, non-condensing
Storage Temperature	-50°C to +50°C
Dimensions	Console: 223 x 69 x 40 mm Sensor Staff: 4 x 450 mm sections Sensor: 170 x 71 mm dia. Weight: console 2.1 kg, sensor and staff assembly 2.2 kg
Integrated GPS	Yes

Precision
GeoSurveys

Hemisphere R220 GPS Receiver Specifications

GPS Sensor	Receiver Type	L1 and L2 RTK with carrier phase	
	Channels	12 L1CA GPS 12 L1P GPS 12 L2P GPS 3 SBAS or 3 additional L1CA GPS	
	Update Rate	10 Hz standard, 20 Hz available	
	Cold Start Time	<60 s	
	Warm Start Time 1	30 s (valid ephemeris)	
	Warm Start Time 2	30 s (almanac and RTC)	
	Hot Start Time	10 s typical (valid ephemeris and RTC)	
	Reacquisition	<1 s	
	Differential Options	SBAS, Autonomous, External RTCM, RTK, OmniSTAR (HP/XP)	
Horizontal Accuracy		RMS (67%)	2DRMS (95%)
	RTK [1, 2]	10 mm + 1 ppm	20 mm+2 ppm
	OmniSTAR HP [1, 3]	0.1 m	0.2 m
	SBAS (WAAS) [1]	0.3 m	0.6 m
	Autonomous, no SA [1]	1.2 m	2.5 m
L-Band Sensor	Channel	Single channel	
	Frequency Range	1530 MHz to 1560 MHz	
	Satellite Selection	Manual or Automatic (based on location)	
	Startup and Satellite Reacquisition Time	15 seconds typical	
Communications	Serial Ports	2 full duplex RS232	
	Baud Rates	4800 – 115200	
	USB Ports	1 Communications, 1 Flash Drive data storage	
	Correction I/O Protocol	Hemisphere GPS proprietary, RTCM v2.3 (DGPS), RTCM v3 (RTK), CMR, CMR+NMEA 0183, Hemisphere GPS binary	
	Timing Output	1 PPS (HCMOS, active high, rising edge sync, 10 kΩ, 10 pF load)	
	Event Marker Input	HCMOS, active low, falling edge sync, 10 kΩ	
Environmental	Operating Temperature	-30°C to +65°C	
	Storage Temperature	-40°C to +85°C	
	Humidity	95% non-condensing	
Power GPS Sensor	Input Voltage Range	8 to 36 VDC	
	Consumption, RTK	<4.9 W (0.40 A @ 12 VDC typical)	
	Consumption, OmniSTAR	<5.5 W (0.46 A @ 12 VDC typical)	

[1] Depends on multipath environment, number of satellites in view, satellite geometry and ionospheric activity.
[2] Depends also on baseline length.
[3] Requires a subscription from OmniSTAR.

Opti-Logic RS800 Rangefinder Laser Altimeter

Accuracy	+/- 1 m on 1x1 m^2 diffuse target with 50% reflectivity, up to 700 m
Resolution	0.2 m
Communication Protocol	RS232-8,N,1
Baud Rate	19200
Data Raw Counts	~200 Hz
Data Calibrated Range	~10 Hz
Calibrated Range Units	Feet, Meters, Yards
Laser	Class I (eye-safe) 905 nm +/- 10 nm
Power	7-9 VDC conditioned required, current draw at full power (~ 1.8 W)
Laser Wavelength	RS100 905 nm +/- 10 nm
Laser Divergence	Vertical axis – 3.5 mrad half-angle divergence; Horizontal axis – 1 mrad half-angle divergence; (Approximate beam footprint at 100 m is 35 cm x 5 cm)
Data Rate	~200 Hz raw counts for un-calibrated operation; ~10 Hz for calibrated operation (averaging algorithm seeks 8 good readings)
Dimensions	32 x 78 x 84 mm (lens face cross section is 32 x 78 mm)
Weight	< 227 g (8 oz)
Casing	RS100/RS400/RS800 units are supplied as OEM modules consisting of an open chassis containing optics and circuit boards. Custom housings can be designed and built on request.

Setra Model 276 Barometric Pressure

Pressure Ranges	600 to 1100 hPa/mb 800 to 1100 hPa/mb 0 to 20 psia
Accuracy	±0.25% FS
Output	0.1 to 5.1 VDC 0.5 to 4.5 VDC
Excitation	12 VDC (9.0 to 14.5) 24 VDC (21.6 to 26.0) 5 VDC (4.9 to 7.1)
Size	2" dia. x 1" (5 cm x 2.5 cm)

Precision
GeoSurveys

Scintrex CS-3 Magnetometer

Operating Principal	Self-oscillating split-beam Cesium Vapor (non-radioactive ^{133}Cs)
Operating Range	15,000 to 105,000 nT
Gradient Tolerance	40,000 nT/meter
Operating Zones	10° to 85° and 95° to 170°
Hemisphere Switching	a) Automatic b) Electronic control actuated by the control voltage levels (TTL/CMOS) c) Manual
Sensitivity	0.0006 nT √Hz rms
Noise Envelope	Typically 0.002 nT P-P, 0.1 to 1 Hz bandwidth
Heading Error	+/- 0.25 nT (inside the optical axis to the field direction angle range 15° to 75° and 105° to 165°)
Absolute Accuracy	<2.5 nT throughout range
Output	a) Continuous signal at the Larmor frequency which is proportional to the magnetic field (proportionality constant 3.49857 Hz/nT) sine wave signal amplitude modulated on the power supply voltage b) Square wave signal at the I/O connector, TTL/CMOS compatible
Information Bandwidth	Only limited by the magnetometer processor used
Sensor Head	Diameter: 63 mm (2.5") Length: 160 mm (6.3") Weight: 1.15 kg (2.6 lb)
Sensor Electronics	Diameter: 63 mm (2.5") Length: 350 mm (13.8") Weight: 1.5 kg (3.3 lb)
Cable, Sensor to Sensor Electronics	3 m (9' 8"), lengths up to 5 m (16' 4") available
Operating Temperature	-40°C to +50°C
Humidity	Up to 100%, splash proof
Supply Power	24 to 35 Volts DC
Supply Current	Approx. 1.5 A at start up, decreasing to 0.5 A at 20°C
Power Up Time	Less than 15 minutes at -30°C

Precision
GeoSurveys

Billingsley TFM100G2 Ultra Miniature Triaxial Fluxgate Magnetometer

Axial Alignment	Orthogonality better than ± 1°
Input Voltage Options	15 to 34 VDC @ 30 mA
Field Measurement Range Options	± 100 µT = ± 10V
Accuracy	± 0.75% of full scale (0.5% typical)
Linearity	± 0.015% of full scale
Sensitivity	100 µV/nT
Scale Factor Temperature Shift	0.007% full scale/°C
Noise	≤12 pT rms/√Hz @ 1 Hz
Output Ripple	3 mV peak to peak @ 2nd harmonic
Analog Output at Zero Field	± 0.025 V
Zero Shift with Temperature	± 0.6 nT/°C
Susceptibility to Perming	± 8 nT shift with ± 5 Gauss applied
Output Impedance	332 Ω ± 5%
Frequency Response	3 dB @ > 500 Hz (to > 4 KHz wide band)
Over Load Recovery	± 5 Gauss slew < 2 milliseconds
Random Vibration	> 20G rms 20 Hz to 2 KHz
Temperature Range	- 55°C to + 85°C
Acceleration	> 60G
Weight	100 g
Size	3.51 cm x 3.23 cm x 8.26 cm
Connector	Chassis mounted 9 pin male "D" type

Precision
GeoSurveys

Pico Envirotec GRS-10 Gamma Spectrometer Specifications

Crystal volume	8.4 litres of NaI(Tl) synthetic downward-looking crystals
Resolution	256/512 channels
Tuning	Automatic using peak determination algorithm
Detector	Digital Peak
Calibration	Fully automated detector
Real Time	Linearization and gain stabilization
Communication	RS232
Detectors	Expandable to 10 detectors and digital peak
Count Rate	Up to 60,000 cps per detector
Count Capacity per channel	65545
Energy detection range:	36 KeV to 3 MeV
Cosmic channel	Above 3 MeV
Upward Shielding	RayShield® non-radioactive shielding on downward-looking crystals
Spectra	Collected spectra of 256/512 channels, internal spectrum resolution 1024
Software	Calibration: High voltage adjustment, linearity correction coefficients calculation, and communication test support Real Time Data Collection: Automatic Gain real time control on natural isotopes, and PC based test and calibration software suite
Sensor	Each box containing two (2) gamma detection NaI(Tl) crystals – each 4.2 liters. (256 cu in.) (approx. 100 x 100 x 650 mm) Total volume of approx. 8.4 litres or 512 cu in with detector electronics
Spectra Stabilization	Real time automatic corrections on radio nuclei: Th, U, K. No implanted sources

Pico Envirotec AGIS data recorder system

(for navigation and geophysical data acquisition)

Functions	Airborne Geophysical Information System (AGIS) with integrated Global Positioning System Receiver (GPS) and all necessary navigation guidance software. Inputs for geophysical sensors - portable gamma ray spectrometer GRS-10/AGRS, MMS4 Magnetometer, Totem 2A EM, A/D converter, temperature probe, humidity probe, barometric pressure probe, and laser altimeter. Output for the multi-parameter PGU (Pilot Guidance Unit)
Display	Touch screen with display of 800 x 600 pixels; customized keypad and operator keyboard. Multi-screen options for real-time viewing of all data inputs, fiducial points, flight line tracking, and GPS channels by operator.
GPS Navigation	12 channel, WAAS/SBAS-enabled
Data Sampling	Sensor dependent
Data Synchronization	Synchronized to GPS position
Data File	PEI Binary data format
Storage	80 GB
Supplied Software	PEIView: Allows fast data Quality Control (QC) Data Format: Geosoft GBN and ASCII output PEIConv: For survey preparation and survey plot after data acquisition
Software	Calibration: High voltage adjustment, linearity correction coefficients calculation, and communication test support Real Time Data Collection: Automatic Gain real time control on natural isotopes and PC based test and calibration software suite
Power Requirements	24 to 32 VDC
Temperature	Operating: -10°C to +55°C; storage: -20°C to +70°C

Precision
GeoSurveys

Appendix B
Digital File Descriptions

- Magnetic database description
- Radiometric database description
- Grids
- Maps

Magnetic Database:

Abbreviations used in the GDB/XYZ files listed below:

CHANNEL	UNITS	DESCRIPTION
X_WGS84	m	UTM Easting – WGS 84 Zone 17N
Y_WGS84	m	UTM Northing – WGS 84 Zone 17N
Lon_deg	Decimal degree	Longitude
Lat_deg	Decimal degree	Latitude
Block_Name		Name of survey block
Date	yyyy/mm/dd	Dates of the survey flight(s) – Local
FLT		Flight Line numbers
LineNo		Line numbers
STL		Number of satellite(s)
GPSfix		1 = non-differential 2 = WAAS/SBAS differential
GPStime	Hours:min:secs	GPS time (UTC)
Geos_m	m	Geoidal separation
GHead_deg	Decimal degree	Heading of the aircraft
XTE_m	m	Cross track error
Galt	m	GPS height – WGS 84 Zone 17N (ASL)
Lalt	m	Laser Altimeter readings (AGL)
DTM	m	Digital Terrain Model
Sample_Density	m	Horizontal distance in meters between adjacent measurement locations; sample frequency is 20 Hz
Speed_km_hr	km/hr	Ground speed of aircraft in km/hr
basemag	nT	Base station temporal data
IGRF_original		International Geomagnetic Reference Field 2015; 12th generation for original survey date
Declin_original	Decimal degree	Calculated declination of magnetic field on original survey date
Inclin_original	Decimal degree	Calculated inclination of magnetic field on original survey date
IGRF_2018		International Geomagnetic Reference Field 2015; 12th generation – Calculated for July 14, 2018
Declin_2018	Decimal degree	Calculated declination of magnetic field on July 14, 2018
Inclin_2018	Decimal degree	Calculated inclination of magnetic field on July 14, 2018
TMI_Original	nT	2016 Total Magnetic Intensity
RMI_Original	nT	2016 Residual Magnetic Intensity
TMI	nT	2016 and 2018 Total Magnetic Intensity
RMI	nT	2016 and 2018 Residual Magnetic Intensity

Radiometric Database:

Abbreviations used in the GDB/XYZ files:

CHANNEL	UNITS	DESCRIPTION
X_WGS84	m	UTM Easting – WGS 84 Zone 17N
Y_WGS84	m	UTM Northing – WGS 84 Zone 17N
Lon_deg	degree	Longitude
Lat_deg	degree	Latitude
Block_Name		Name of survey block
Date	yyyy/mm/dd	Dates of the survey flight(s) – Local
FLT		Flight numbers
LineNo		Line numbers
STL		Number of satellite(s)
GPStime	Hours:min:secs	GPS time (UTC)
Geos_m	m	Geoidal separation
GPSFix		1 = non-differential 2 = WAAS/SBAS differential
GHead_deg	degree	Heading of the aircraft
XTE_m	m	Flight line cross distance
Galt	m	GPS height – WGS 84 Zone 17N (ASL)
Lalt	m	Laser Altimeter readings (AGL)
DTM	m	Digital Terrain Model
Sample_Density	m	Horizontal distance in metres between adjacent measurement locations; sample frequency is 20 measurements per second
Speed_km_hr	km/hr	Ground speed of aircraft in km/hr
BaroSTP_kPa	KiloPascal	Barometric Altitude (Press and Temp Corrected)
Temp_degC	Degrees C	Air Temperature
Press_kPa	KiloPascal	Atmospheric Pressure
COSFILT	counts/sec	Spectrometer - Filtered Cosmic
UPUFILT	counts/sec	Spectrometer – Filtered Upward Uranium
Kcor	%	Concentration in Percentage - Potassium
Thcor	ppm	Equivalent Concentration - Thorium
Ucor	ppm	Equivalent Concentration - Uranium
TCcor	nGy/hour	Total Count
TCexp	µR/hour	Exposure Rate
KThratio		Spectrometer –%K/eTh ratio
KUratio		Spectrometer –%K/eU ratio
ThKratio		Spectrometer – eTh/%K ratio
ThUratio		Spectrometer – eTh/eU ratio
UKratio		Spectrometer – eU/%K ratio
UThratio		Spectrometer – eU/eTh ratio
Kcor_16_18	%	Concentration in Percentage – Potassium (2016 and 2018 merged and leveled)
Thcor_16_18	ppm	Equivalent Concentration – Thorium (2016 and 2018 merged and leveled)
Ucor_16_18	ppm	Equivalent Concentration – Uranium (2016 and 2018 merged and leveled)

Precision GeoSurveys

Radiometric Database (continued):

CHANNEL	UNITS	DESCRIPTION
TCcor_16_18	nGy/hour	Total Count (2016 and 2018 merged and leveled)
TCexp_16_18	µR/hour	Exposure Rate (2016 and 2018 merged and leveled)
KThratio_16_18		Spectrometer –%K/eTh ratio (2016 and 2018 merged and leveled)
KUratio_16_18		Spectrometer –%K/eU ratio (2016 and 2018 merged and leveled)
ThKratio_16_18		Spectrometer – eTh/%K ratio (2016 and 2018 merged and leveled)
ThUratio_16_18		Spectrometer – eTh/eU ratio (2016 and 2018 merged and leveled)
UKratio_16_18		Spectrometer – eU/%K ratio (2016 and 2018 merged and leveled)
UThratio_16_18		Spectrometer – eU/eTh ratio (2016 and 2018 merged and leveled)

Grids: 2018 White Reserve Survey Block WGS 84 Datum, Zone 17N, cell size at 25 m

FILE NAME	DESCRIPTION
2018_WhiteReserve_DTM_25m.grd	Digital Terrain Model gridded at 25 m cell size
2018_WhiteReserve_TMI_25m.grd	Total Magnetic Intensity gridded at 25 m cell size
2018_WhiteReserve_RMI_25m.grd	Residual Magnetic Intensity gridded at 25 m cell size
2018_WhiteReserve_CVG_25m.grd	Calculated Vertical Gradient of RMI gridded at 25 m cell size
2018_WhiteReserve_RTP_25m.grd	Reduced to Magnetic Pole of RMI gridded at 25 m cell size
2018_WhiteReserve_1VD_25m.grd	First Vertical Derivative of RTP gridded at 25 m cell size
2018_WhiteReserve_CHG_25m.grd	Calculated Horizontal Gradient of RMI gridded at 25 m cell size
2018_WhiteReserve_Kcor_25m.grd	Potassium (%K) - concentration in percentage gridded at 25 m cell size
2018_WhiteReserve_Thcor_25m.grd	Thorium (eTh) – equivalent concentration gridded at 25 m cell size
2018_WhiteReserve_Ucor_25m.grd	Uranium (eU) – equivalent concentration gridded at 25 m cell size
2018_WhiteReserve_TCcor_25m.grd	Total Count (TC) gridded at 25 m cell size
2018_WhiteReserve_TCexp_25m.grd	Total Count (TCexp) – exposure rate gridded at 25 m cell size
2018_WhiteReserve_KThratio_25m.grd	Potassium over Thorium ratio (%K/eTh) gridded at 25 m cell size
2018_WhiteReserve_KUratio_25m.grd	Potassium over Uranium ratio (%K/eU) gridded at 25 m cell size
2018_WhiteReserve_UThratio_25m.grd	Uranium over Thorium ratio (eU/eTh) gridded at 25 m cell size
2018_WhiteReserve_UKratio_25m.grd	Uranium over Potassium ratio (eU/%K) gridded at 25 m cell size
2018_WhiteReserve_ThKratio_25m.grd	Thorium over Potassium ratio (eTh/%K) gridded at 25 m cell size
2018_WhiteReserve_ThUratio_25m.grd	Thorium over Uranium ratio (eTh/eU) gridded at 25 m cell size

Precision
GeoSurveys

<u>Grids:</u> 2016 and 2018 White Reserve Survey Blocks, WGS 84 Datum, Zone 17N, cell size at 25 m

FILE NAME	DESCRIPTION
2016_2018_WhiteReserve_DTM_25m.grd	Digital Terrain Model gridded at 25 m cell size
2016_2018_WhiteReserve_TMI_25m.grd	Total Magnetic Intensity gridded at 25 m cell size
2016_2018_WhiteReserve_RMI_25m.grd	Residual Magnetic Intensity gridded at 25 m cell size
2016_2018_WhiteReserve_CVG_25m.grd	Calculated Vertical Gradient of RMI gridded at 25 m cell size
2016_2018_WhiteReserve_RTP_25m.grd	Reduced to Magnetic Pole of RMI gridded at 25 m cell size
2016_2018_WhiteReserve_1VD_25m.grd	First Vertical Derivative of RTP gridded at 25 m cell size
2016_2018_WhiteReserve_CHG_25m.grd	Calculated Horizontal Gradient of RMI gridded at 25 m cell size
2016_2018_WhiteReserve_Kcor_25m.grd	Potassium (%K) - concentration in percentage gridded at 25 m cell size
2016_2018_WhiteReserve_Thcor_25m.grd	Thorium (eTh) – equivalent concentration gridded at 25 m cell size
2016_2018_WhiteReserve_Ucor_25m.grd	Uranium (eU) – equivalent concentration gridded at 25 m cell size
2016_2018_WhiteReserve_TCcor_25m.grd	Total Count (TC) gridded at 25 m cell size
2016_2018_WhiteReserve_TCexp_25m.grd	Total Count (TCexp) – exposure rate gridded at 25 m cell size
2016_2018_WhiteReserve_KThratio_25m.grd	Potassium over Thorium ratio (%K/eTh) gridded at 25 m cell size
2016_2018_WhiteReserve_KUratio_25m.grd	Potassium over Uranium ratio (%K/eU) gridded at 25 m cell size
2016_2018_WhiteReserve_UThratio_25m.grd	Uranium over Thorium ratio (eU/eTh) gridded at 25 m cell size
2016_2018_WhiteReserve_UKratio_25m.grd	Uranium over Potassium ratio (eU/%K) gridded at 25 m cell size
2016_2018_WhiteReserve_ThKratio_25m.grd	Thorium over Potassium ratio (eTh/%K) gridded at 25 m cell size
2016_2018_WhiteReserve_ThUratio_25m.grd	Thorium over Uranium ratio (eTh/eU) gridded at 25 m cell size

<u>Maps:</u> 2016 and 2018 White Reserve Survey Blocks, WGS 84 Datum, Zone 17N (jpegs and pdfs)

FILE NAME	DESCRIPTION
2016_2018_WhiteReserve_ActualFlightLines	Plotted actual flown flight lines
2016_2018_WhiteReserve_DTM_25m	Digital Terrain Model gridded at 25 m cell size
2016_2018_WhiteReserve_TMI_wFL_25m	Total Magnetic Intensity gridded at 25 m cell size with actual flight lines
2016_2018_WhiteReserve_TMI_25m	Total Magnetic Intensity gridded at 25 m cell size
2016_2018_WhiteReserve_RMI_25m	Residual Magnetic Intensity gridded at 25 m cell size
2016_2018_WhiteReserve_CVG_25m	Calculated Vertical Gradient of RMI gridded at 25 m cell size
2016_2018_WhiteReserve_RTP_25m	Reduced to Magnetic Pole of RMI gridded at 25 m cell size
2016_2018_WhiteReserve_1VD_25m	First Vertical Derivative of RTP gridded at 25 m cell size
2016_2018_WhiteReserve_CHG_25m	Calculated Horizontal Gradient of RMI gridded at 25 m cell size
2016_2018_WhiteReserve_Kcor_25m	Potassium (%K) - concentration in percentage gridded at 25 m cell size
2016_2018_WhiteReserve_Thcor_25m	Thorium (eTh) – equivalent concentration gridded at 25 m cell size
2016_2018_WhiteReserve_Ucor_25m	Uranium (eU) – equivalent concentration gridded at 25 m cell size
2016_2018_WhiteReserve_TCcor_25m	Total Count (TC) gridded at 25 m cell size
2016_2018_WhiteReserve_TCexp_25m	Total Count (TCexp) – exposure rate gridded at 25 m cell size
2016_2018_WhiteReserve_KThratio_25m	Potassium over Thorium ratio (%K/eTh) gridded at 25 m cell size
2016_2018_WhiteReserve_KUratio_25m	Potassium over Uranium ratio (%K/eU) gridded at 25 m cell size
2016_2018_WhiteReserve_UThratio_25m	Uranium over Thorium ratio (eU/eTh) gridded at 25 m cell size
2016_2018_WhiteReserve_UKratio_25m	Uranium over Potassium ratio (eU/%K) gridded at 25 m cell size
2016_2018_WhiteReserve_ThKratio_25m	Thorium over Potassium ratio (eTh/%K) gridded at 25 m cell size
2016_2018_WhiteReserve_ThUratio_25m	Thorium over Uranium ratio (eTh/eU) gridded at 25 m cell size
2016_2018_WhiteReserve_TernaryMap_25m	Displaying ratios of all three elements (%K, eTh, eU)

precision
GeoSurveys

Plates
2016 and 2018 White Reserve Survey Blocks
Scale 1:45,000

- Plate 1: 2016 and 2018 White Reserve - Actual Flight Lines (FL)
- Plate 2: 2016 and 2018 White Reserve - Digital Terrain Model (DTM)
- Plate 3: 2016 and 2018 White Reserve - Total Magnetic Intensity with Actual Flight Lines (TMI_wFL)
- Plate 4: 2016 and 2018 White Reserve - Total Magnetic Intensity (TMI)
- Plate 5: 2016 and 2018 White Reserve - Residual Magnetic Intensity (RMI)
- Plate 6: 2016 and 2018 White Reserve - Calculated Vertical Gradient (CVG) of RMI
- Plate 7: 2016 and 2018 White Reserve - Reduced to Magnetic Pole (RTP) of RMI
- Plate 8: 2016 and 2018 White Reserve - First Vertical Derivative (1VD) of RTP
- Plate 9: 2016 and 2018 White Reserve - Calculated Horizontal Gradient (CHG) of RMI
- Plate 10: 2016 and 2018 White Reserve - Potassium – Percentage (%K)
- Plate 11: 2016 and 2018 White Reserve - Thorium – Equivalent Concentration (eTh)
- Plate 12: 2016 and 2018 White Reserve - Uranium – Equivalent Concentration (eU)
- Plate 13: 2016 and 2018 White Reserve - Total Count (TC)
- Plate 14: 2016 and 2018 White Reserve - Total Count – Exposure Rate (TCexp)
- Plate 15: 2016 and 2018 White Reserve - Potassium over Thorium Ratio (%K/eTh)
- Plate 16: 2016 and 2018 White Reserve - Potassium over Uranium Ratio (%K/eU)
- Plate 17: 2016 and 2018 White Reserve - Uranium over Thorium Ratio (eU/eTh)
- Plate 18: 2016 and 2018 White Reserve - Uranium over Potassium Ratio (eU/%K)
- Plate 19: 2016 and 2018 White Reserve - Thorium over Potassium Ratio (eTh/%K)
- Plate 20: 2016 and 2018 White Reserve - Thorium over Uranium Ratio (eTh/eU)
- Plate 21: 2016 and 2018 White Reserve - Ternary Map (TM)

White Reserve Airborne Grid

WILLET

BARBER

SPEIGHT

BANKS

Grid cell values (left to right, top to bottom):

310706 / 343921, 220294 / 321010, 152400 / 154867, 272903 / 154780, 208123, 302645, 154825, 320699, 266724, 200109, 302605, 208886 / 302604, 208885, 220944, 200827

171420, 125594, 208212, 125593, 100085, 274198, 266766, 100051, 274147, 142002, 266725, 302606, 503005

200182, 125595, 200181, 274735, 170885, 266767, 154826, 322863, 125009, 100052, 266726, 125008, 503006

154894, 208744, 286908, 266818, 310675, 125563, 142056, 115719, 310690, 142075, 286875, 115737, 503007

100144, 274767, 274766, 227610, 274199, 322910, 125564, 286863, 274214, 100104, 115738, 154852 / 240855, 128159, 295483, 210947, 140190

100145, 274768, 286910, 286909, 142057, 220270, 227554, 274200, 115739, 154853, 266796, 240856 / 227570, 248356, 314923, 335792, 310863, 310862, 188080

115716, 274197, 100083, 170884, 227551, 142059, 142058, 208179, 142076

266765, 322908, 266764, 115717, 286859, 310711, 100126, 286895, 142741

310674, 208176, 125562, 302644, 286860, 302683, 323450, 125599, 228242

200111, 142008, 142007, 142006, 274093, 286236, 226948, 322821, 275394

142009, 286289, 274151, 200112, 100013, 208080, 266158, 226949, 275395

154786, 286800, 125015, 100057, 320359, 226950, 286238, 286237, 275396

539374, 154788, 125016, 154787, 266730, 274094, 154222, 286239, 266159, 155499

266774, 310677, 266773, 208180, 286364, 274095, 200057, 304070

125565, 227557, 227556, 170886, 142062, 142081, 154857, 220241

539377, 266775, 208181, 154830, 227558, 200149, 142082, 154858, 208152, 154803

302649, 286865, 227559, 100088, 154831, 323438, 274730, 200125

539379, 201212, 344339, 190109, 238228, 338081, 278454, 119770, 176557, 104493

Legend

- Operational_Cell_Claims_BMR_WhiteReserve
- MENDM_Township_Boundaries
- WhiteReserve-2018_Lidar_Survey
- Operational_Alienations
- Non_Mining_Land_Tenure
- Mining_Land_Tenure

1 centimeter = 110 meters

0 375 750 1,500 2,250 3,000 Meters

N / S / E / W (compass)

Sources: Esri, HERE, Garmin, Intermap, increment P Corp., GEBCO, USGS, FAO, NPS, NRCAN, GeoBase, IGN, Kadaster NL, Ordnance Survey, Esri Japan, METI, Esri China (Hong Kong), OpenStreetMap contributors, and the GIS User Community